We thank the reviewers for their valuable and thoughtful comments and suggestions. Most of them have been incorporated in the manuscript. The comments of the reviewers are presented in italic and the line number given refers to the ms version. Text now inserted in the manuscript is given in blue.

General remarks:
The criticized fit of diapycnal diffusivity with water depth is not applied anymore. The regional mean diffusivity is used instead for those stations without microstructure data. This change made a recalculation of the upwelling velocities necessary, so all figures and some numbers in the paper have been modified. The main pattern of upwelling and thus the main conclusions of the paper remained unchanged.

Surfactants during cruise M91 have been observed by 'eye'. Meanwhile, some discussion papers dealing with this issue have been published. One of these is cited and we think it underlines the existence of the surface films and its influence on the gas exchange velocity.

Eq.1: The first term of eq.1 (DC1/Dt) has wrong units, it would need to be multiplied with the depth of the mixed layer. In order not to introduce another quantity in eq.1, the term DC1/Dt (which is assumed to be zero anyway) has been omitted.

Table 1:
The error given for C2 (0.25%) is wrong, it should be 0.2% as is noted in the text and was used for the error calculation. The values in the lines for the Peruvian and Mauritanian upwelling have been changed by mistake. This is now corrected, and the values in table 1 were recalculated anyway due to the above mentioned change in the diapycnal diffusivity at some data points.

Reviewer #1:
1. Page 3. The discussion of 3He is not quite correct. While the Pacific Mid-Ocean Ridges are very active, the Atlantic MOR emits substantial 3He as well. Likely the N-S gradient there results from the fact that the N Atlantic ventilates 3He-free water. In any event, this discussion really is not relevant to the paper. I would drop it.
The discussion of 3He has been shortened.

2. Page 3. "They are, however, much too small to be measured directly, but need to be inferred either from divergence of the wind field or with the helium method,". Rather than helium method, one should say trace methods, of which 3He and 7Be are two. Do a reference search of these other methods.
The term 'tracer methods' is introduced and the different methods listed with literature references.

3. Page 5. Drop lines 22-25. This adds nothing particularly in context of the above comment #1.
We did not drop these lines, as we think it is important to point to the differences in the surface concentration of 3He between the Peruvian and Mauritanian upwelling.

4. *Page 6. Top line: "distinguish between advective and diffusive 3He fluxes" change to „distinguish between advective and diffusive vertical..."(add „vertical").*
Done.

5. Page 7. Equation 1. This formulation is not correct as it leaves out horizontal terms. The authors on page 17 even mention this as a possible effect. One may ignore the term but one should say as much.
We admit that the horizontal terms are left out. However, this is done in all publications using 1-D box models (Klein and Rhein (2004), Rhein et al. (2010), Kadko et al. (2011), Haskell et al. (2015)).

It is now explicitely written after Eq. 1 that the horizontal terms are neglected or that the approach is valid in a Lagrangian framework: All these models neglect horizontal advection,~i.~e it is assumed that changes of the respective tracer in the mixed layer is dominated by vertical processes. Another interpretation is that Eq.~1 is valid in a Lagrangian coordinate system moving with the surface patch (box 1), as long as the lower box 2 moves with a similar velocity and horizontal mixing is small.

6. Figure 3: Is this valid? Is there a theoretical justification of this approach? Any references? There is tremendous scatter in the figure - is it really useful? Also, is it valid to put data from Peru and Mauritania in the same figure - do different mechanics apply because of shelf/coast differences?? Perhaps this figure can be dropped.
This figure has been dropped, and the fit between diffusivity and water depth is not used in the revised version of the paper.

7. page 9: lines 20 onward should be dropped. It is speculative and adds needless length and words to the paper.
Done.

8. Page 12, line 4. "Here, no decrease in offshore direction of the upwelling velocity can be observed". This is not true - one can see a decrease. The following sentence does not match the data in Figure 4 well either.
The quoted sentence has been dropped. The next sentence has been changed to 'Another region with strong upwelling further south at 12-14°S is restricted to the coast. Around 10°S and south of 15°S the upwelling is weak or even vanishing'.

9. Page 12, Lines12-14. An important test that the authors should do, to convince themselves that their upwelling numbers are real (I am talking about off shore, or unexpected points of upwelling, or in cases when c1-c2 is quite small, in particular) is to plot upwelling values against temperature and/or PO4. A near-linear plot should result if the upwelling is real. I am surprised the authors did not do this.
We agree that this is a good test, and it has been done, but it is not shown in the paper. The results are inconclusive: The correlation between upwelling and PO4 is positive, for upwelling and temperature negative, as it should be. However, these correlations are only significant for the M91 cruise. One reason could be offshore transport, and PO4 might have a longer 'residence time' in the mixed layer compared to helium-3. SST off Mauritania is also influenced by horizontal advection and the front related with the Canary Current.

10. Page 16, lines 16-20. Within the error bars the derived W values are no different from one another. There is no "significantly larger values". This is very careless writing and interpretation.
We agree that this formulation is not appropriate. It is now written 'All these numbers, however, agree within their error bars.'

11. Page 16: I disagree that for the Peruvian coastal region, the differences between Whe and Wwind are significant. Taking into account the error bars, these values are within a factor of 2 of each other. This is insignificant.
We think that this difference is significamt, despite of the large error bars. The student t-factor for 90% and n=18 (as 19 =n+1 velocities are used for the mean) is 1.33. The mean Whe is 2.7 +-0.6. Multiplying 0.6 with 1.33 gives 0.8, i.e.the probability for the mean Whe being smaller than 1.9 is 10%. Wwind is 1.2 +-0.2, so the probability for the mean of Wwind being larger than 1.5 is 10%. That means the probability for the two mean values being equal is less than 1%.
Then calling into account an unsubstantiated reason--surface films--to explain this small difference is absurd. There are no references for this phenomena presented for Peru so it is simply a waste

of time, words and space. This whole discussion should be removed, and the corresponding figures adjusted (e.g. remove figure 6). This and the previous comment indicate why this paper is too long and rambling.
The presence of surfactants off Peru during the cruise M91 have been observed by two of the coauthors by eye. We regret not to have mentioned this in the text, so the impression could arise, that the surfactants are an 'unsubstantiated' topic. Meanwhile, a paper has been published (Kiefhaber et al., 2015), which shows the effect of surfactants in reducing the wave slope during cruise M91. This paper is now taken up in the manuscript:
These films have been observed on cruise M91, and their damping behaviour onsurface waves have been shown in Kiefhaber et al.(2015). There, the observed mean square slope of the waves was found to be overestimated by the parameterization for clean water. Mostmeasurements are in the range spanned by clean water and slick parameterizations.

12. Page 17. This discussion of offshore signal advection is significant, but ironically, this important point is not developed in the paper, and it should be part of equation 1. I am wondering if this effect could account for some of the differences the authors attempt to describe.
Offshore advection might be important, but it is hard to quantify without moorings or shipboard sections that run parallel to the coast.
As written above and in the text, the 1-D box models used in the literature do not contain the horizontal transport, and eq. 1 is valid in a Lagrangian coordinate system moving with the surface patch.

13. page 19. The discussion here is hard to follow, as well as the interpretation of Figure 8 and 9. I see no proof that eddies are responsible for upwelling from these data. In the abstract, it is stated that eddy induced upwelling "might" be responsible for the offshore wind driven upwelling. However by the time we come to the conclusion (last paragraph of the paper) the authors state the importance of eddies in their work. There is no evidence to support this. This is very highly overstated. Experimentally, one would have to go to an eddy in real time and make these measurements.
We agree that it would be best to follow an eddy and try to infer the vertical velocity inside, outside and at the edge. Unfortunately this has not been done on the cruises presented here. The importance of eddies, especially for nutrient transport, is cited from the literature and not solely based on this study, as the data presented here are not completely stringent in that respect. We changed the Figures 8 and 9 and the description in the text. Now not showing the vertical velocity is shown, but the difference between Whe and Wwind, i.e. the part of the vertical velocity which might be explained by eddies. We think, the influence on SLA for the offshore upwelling becomes a bit clearer now. In Fig.9, the coastal data points have been removed, as for them no influence of SLA on the upwelling can be deduced.

14. page 20: As stated earlier there is no justification to use a reduced gas flux upwelling.

Technical Corrections:
1. Page 3,line 16: "based on Beryllium isotopes and was used by" change to "based on the isotope 7Be used by"
This paragraph has been reformulated, "Beryllium isotopes" has been changed to "7Be".

2. Page 4, line 6: "We will thus compare the Ekman and helium derived vertical velocities". Remove this sentence as it is redundant to the following lines.
Done.

3. Figure symbols. The color scheme on some of the figures (filled circles) is hard to read. Specifically the orange and red circles are difficult to distinguish, particularly on the small figures.

The orange color has been made lighter and the red color darker to make them better distinguishable.

Can the figures in figure 4 be made larger?
The figure has been made larger as a whole.

4. There are many spelling errors that must be checked.
Sorry for that, but none of the authors is a native speaker. We found some spelling errors that have been corrected.

5. Page 4, line 26. Change "water probes" to "water subsamples".
Done.

Reviewer #2:
Pg. 20, Line 6: You do not specify what, 'Direct observations' of vertical diffusivity are. Please say "microstructure-based estimates of vertical diffusivity." Technically, the microstructure approach is just as 'indirect' as a geochemical tracer, as you state in the first sentence. The instrument measures small-scale shear velocity and equates it to turbulent kinetic energy dissipation, which under the assumption of isotropy, can be related to diffusivity.
"direct observations" has been replaced with "microstructure based".

Line 11: You describe the agreement between the wind-based and He-based estimates are "fairly good." This is too subjective for the reader to interpret. Also on Line 14, you state that eddies "might be" responsible for upwelling. This is also too ambiguous for an abstract, in my opinion. Overall, I think the abstract should be re-written.
We agree, "fairly good" is now omitted. Parts of the abstract have been re-written.

Pg. 21, Line 6, 11, 15 (Introduction paragraph 2): There are a couple of points I'd like to make here. 1.) Other geochemical budgets have been used to estimate upwelling other than He, even in the same locations as this study. Please at least list some and cite authors (temperature, AOU, pCO2, 14C, 7Be - Broecker, Peng, Toggweiler, Quay, Kadko...). Haskell et al., 2015 was even in the Peruvian upwelling system. If this is the only paper one reads, then one might think there are only two to three approaches used...
These papers and methods are now listed in the introduction.

2.) Were Klein and Rhein, 2004 and Rhein et al., 2010 the first to use 3He as a tracer for upwelling? Why only cite them?
We do not know any other papers using 3He to directly estimate upwelling velocities in the ocean.

3.) 3He input into the Atlantic is not only from transport,
but the way it is written, it kind of sounds that way. Please at least state that there are inputs at the ridges along the MAR too. Also, is the overall amount of 3He input still debated? I think this paragraph is over simplified and should be re-written. The introduction in general does not read well and deserves some more thought, in my opinion.
This paragraph has been shortened, as was suggested by reviewer#1, and mid-ocean ridges in general are now mentioned as source of 3He.

Pg. 25, Line 10: Even though your model is very similar to the one used by Rhein et al., 2010, I think it would still be useful to start with a brief description of it. It is almost like you are assuming the reader will be familiar with the Rhein et al. Paper. Maybe just one sentence more that sets up

the two-box model...
The box model is now described in more detail:
This model only has a vertical dimension with two boxes. The upper box 1 represents the mixed layer, where gas exchange with the atmosphere takes place. The lower box 2 exchanges properties with box 1 by advective and diffusive vertical fluxes. This box thus supplies the upwelling water enriched in ^{3}He.

Pg. 26, Line 13: Taking the mean 3He value in 5 to 25m below the ML is arbitrary, but is necessary to make this calculation. If you do this, it is only appropriate to be very clear about the uncertainty added by making this assumption because this depth range must equate to a large range in 3He. Can you please list for each upwelling velocity reported, the exact depth range you use for the mean in the deeper box? Also, please give an estimate of the uncertainty added when taking each of these means.
For each profile, the depth range between 5 and 25 m below the mixed layer (at this profile) is used to calculate the helium-3 value of box 2. Reporting this depth for each profile would need to list more than 100 depth ranges, which we think is not practicable. The uncertainty for helium-3 in box 2 is dominated by the uncertainty of the helium measurements. This can be seen by following calculation: The mean gradient of helium-3 in box 2 is about 0.02%/m. Assuming a constant increase of helium-3 by this number over 20 m leads to a standard deviation of the helium-3 concentration by ~0.1%, smaller than the measurement error of 0.2%.

Pg. 27, Line 7 and Fig. 3: I am somewhat lost here. Why use water depth? Thisseems arbitrary and deserves an explanation. I understand that microstructure measurements have demonstrated that there is higher diffusivity near surface and bottom boundaries in the water column, but there has not been any general definitive relation reported that I know of since microstructure-based energy dissipation measurements range orders of magnitude over only meter length scales and certainly through time at any given location. The fit to the data does not seem very good. You report the mean deviation to the fit as 30%, but the range of values is almost 4 orders of magnitude and by eye, there does not appear to be much of a relation. I would think that in order to use a relation between depth and diffusivity, one must estimate diffusivity through time at one location for a very long time to obtain the necessary statistical precision...
The fit and figure 3 have been removed. For the profiles without microstructure data, the regional mean value is now used. This text has been changed accordingly.

Line 21: How about no upwelling or downwelling? Why do you not mention this as a possibility?
Reviewer #1 suggested to drop this discussion, which we did.

Pg. 28, Line 15: Why are you comparing temperatures of upwelled water? Why should they be compared at different locations? I don't see the point to this paragraph.
We agree and dropped this description of temperature distribution.

Pg. 29, Line 5: It sounds like you are saying that horizontal effects dominate the signal. But that goes against your whole approach...
Of course gradients, especially in offshore direction, exist. So long the water does not move too fast along these gradients (i.e. on/offshore instead off alongshore), vertical processes are dominating. The existence of these gradients already illustrates that the velocity in on/offshore directions is relatively small, otherwise the gradients would disappear, as conservative quantities as temperature and 3He are constant along streamlines.

Line 17: This warrants more of a discussion. If you set negative values to zero, you are neglecting downwelling, which is likely what's happening here, especially given the observations you report on page 27. Please discuss this.

The description from page 27 has been dropped. If there was upwelling, it is below the surface, as the upper isolines are moving upward, and the lower isolines are moving downward. You are right, downwelling might occur, also at the base of the mixed layer. We think it is hard to determine by our approach. Additionally, we are mainly interested in the upwelling, not in the total vertical flux, and only for the latter downwelling would have to be taken into account.

Pg. 31, Line 1: So, you neglect the uncertainty in the 3He gradient, even though you use a different depth range for each location. This introduces a huge uncertainty, probably around 50%. I'd like to see an estimate. Uncertainty in gas exchange is typically around 30%, which you neglect, and the uncertainty in Kz is, as you say, 100%. So, w should be at least 100% uncertain. On Line 29, you say the uncertainty is 81% and 98% or each location. This sounds about right, but a little low. But why do you report this in he table?
We don't see why a different depth range for each location introduces a large uncertainty. This depth range is the same for which the diffusivity is calculated and for which the derived vertical velocity is valid. A similar procedure has also been applied e.g. in Tanhua at al.(2015).
If Kz is uncertain by 100%, this does not imply that w is also uncertain by 100%. The reason is that w is not proportional to Kz (see eq.1). In most cases, the Kz term in eq.1 is smaller than the gas exchange, thus the resulting error from Kz for w is smaller than 100%. The exact error of w due to the 100% error of Kz is given in table 1.
For gas exchange, we now adopt the uncertainty of 30%.
We added a line to table 1 which gives the total error of Whe, i.e. the number that is given in the text.

Line 12: Why take half the range of values to estimate uncertainty in w? Why not the whole range? Regardless, uncertainty should still be at least 100%...
The uncertainty is calculated as (wmax-wmin)/2. wmax can be interpreted as wmean +std(wmean), and wmin as wmean-std(wmean). Solving for std(wmean) gives std(wmean)=(wmax-wmin)/2.

Pg. 32, Line 17: I'm not sure it is appropriate to use the mean density in the 500m below the mixed layer here. I am unaware of any literature that estimates the depth of upwelled source water to originate deeper than about 200m, especially as close to the continent as this study. If you were to use a lower density, how would that affect the result?
The mean density over the depth range from the mixed layer boundary down to 500m below the mixed layer is not so different from the density at a depth of ~200m. Using this broad depth range avoids to specifiy a certain depth, which is not well known and might even be varaiable in space and time. The Rossby radius a, which depends on this density, would change, so the coastal wind derived upwelling inferred from equation 6 would also change. A smaller Rossby radius (i.e. a smaller density difference) would lead to a higher vertical velocity directly of the coast and a faster decrease in offshore direction. When integrating the vertical velocity over several Rossby radii (which is done when calculating the mean over all coastal data), this difference almost cancels out. The mean coastal upwelling is thus almost not influenced by the exact choice of the density of the lower layer. This is mentioned in the text.
The magnitude of the wind driven coastal upwelling velocities at each station depends on the choice of the Rossby radius a in Eq.~(6). The total vertical transport integrated over the coastal area, i.~e.~ a distance of several Rossby radii, is almost independent from a.

Pg. 34, Line 19: This statement is true, but why don' you say something about he Spring? This is when you should have the highest variation in upwelling velocity, no? So, it is not that surprising that Winter and Summer are not that different. Please comment on this.
Upwelling off Mauritania is in general high during winter/spring (e.g. Hagen 2001, Carr et al.2003), whereas in summer/autumn a minimum would be expected. Unfortunately we do not have spring data, we cannot say anything about that season. The upwelling during summer would be expected

to be lower than during winter.

Line 27: The connection to surfactants comes out of nowhere. What evidence do you have for suggesting this as a possible explanation for your observations? It does not seem like you have enough information to make this statement. I suggest deleting this part of the discussion. This section is already very long.
Unfortunately we did not mention that two of the coauthors observed surfactamts on cruise M91 by eye. So the impression could arise that the surfactants topic comes 'out of nowhere'. Meanwhile, a paper has been puiblished (Kiefhaber et al., 2015), which shows the influence of surfactants on the wave slope off Peru during cruise M91.
These films have been observed on cruise M91, and their damping behaviour onsurface waves have been shown in Kiefhaber et al.(2015). There, the observed mean square slope of the waves was found to be overestimated by the parameterization for clean water. Mostmeasurements are in the range spanned by clean water and slick parameterizations.

Pg. 38, Line 1: If eddy-induced upwelling is occurring, is it affecting the region off Peru, off Africa, or both? The sea-surface anomaly does not look the same everywhere... If it does affect both regions, do you have an explanation for why it is the same in these very different systems? This is an important point to make.
The eddies obey the same physical laws everywhere, so their influence on the vertical velocity should also be similar between regions (there is a dependence e.g. on the Coriolis parameter
f and stratification, but these are similar (f has the opposite sign, but similar magnitude off Peru and off Mauritania) for both regions.

Line 8: While it is appropriate to calculate the nutrient fluxes in an identical manner to the He fluxes, I am still somewhat concerned with the method. The mean value in a box beneath the mixed layer (of arbitrary size) is not the value of water that enters the euphotic zone. I think if you are going to make this calculation, you should discuss the aspect of choosing the nutrient content of upwelled water in more detail.
You are right that the nutrient concentration at the base of the euphotic zone would be more suitable for calculating the nutrient flux. We added a paragraph on the difference between the vertical velocity and the nutrient concentration at the base of he mixed layer and the base of the euphotic zone.
The important parameter for primary production is the nutrient flux at the base of the euphotic zone. This zone is typically deeper than the mixed layer for which the fluxes in this study are calculated. However, neither the depth of the euphotic zone nore the vertical velocity w at this location is precisely known. Typically, the euphotic zone is deeper than the relatively shallow mixed layers observed in the upwelling regions.'Assuming a decrease of w with depth and an increase of nutrient concentrations, these two gradients are counteracting in their effect on the nutrient flux, so the numbers presented here are considered as approximations of the nutrient flux in the euphotic zone.

Pg. 38-40: The discussion of nutrient fluxes is quite long. You may want to shorten it.
The paragraph on the comparison between NPP and NCP has been dropped.

Pg. 41, Line 2: Why not compare these values to Haskell et al. (2015)? They estimate upwelling velocity using a 7Be budget very close to your study location off Peru.
Both the paper by Haskell et al.(2015) as well as a new paper by Tanhua and al.(2015) are now included in the discussion.

Pg. 41, Line 9: Again, why invoke surfactants? I think you should delete this statement unless you have measurements that they were present.
The paper by Kiefhaber at al. (2015) is now cited here, and the text has been modified accordingly.

For the Mauritanian area, Tanhua and Liu (2015) have calculated upwelling velocities using the same box model as here, but CFC-12 and SF_6 as tracers. For a winter and spring cruise, the vertical velocities are between 0 and 11 * 10^{-5} m s^{-1}, comparable with our results. For the summer cruise M68/3, Toste and Liu (2015) find no indications forupwelling. Their data set, however, only contains a few stations along 18°N. Our coastal stations along that line also have low vertical velocities (between 0 and 2 * 10^{-5} m s^{-1},whereas directly north and around 20°N the helium derived upwelling exceeds 3 * 10^{-5} m s^{-1}.
Haskell et al.(2015) investigate upwelling in the Eastern Tropical South Pacific at a few stations based on the ^{7}Be method.Their vertical velocities are also in the order of 10^{-5} m s^{-1}(0-3 * 10^{-5} m s^{-1}), whereby the maximum value of 3 * 10^{-5} m s^{-1}might be due to 'anomalous 7Be easurements'.

Pg. 41, Line 12: Please show the uncertainty in every figure and table.
The uncertainty is given in all tables and in figure 4 (former figure 5). For the figures showing a larger number of data points, the uncertainty is now noted in the legend.

Pg. 41, Line 21: Here, you may want to focus on the spatial areas covered by using each approach. Given the real uncertainty in the He approach, they agree pretty well in general.
They agree pretty well despite of the offshore regions of cruises M68/3 and ATA3, which have the high WHe value of 10−5 m/s and are discussed here.

Pg. 42, Line 14: Not sure you should end with this. Does this study really show that eddies are responsible? You merely suggest that they are with some evidence to support this idea, but this statement does not reflect this.
The eddy/nutrient discussion has been shifted to the nutrient chapter, and the last sentence has been deleted.

Tables 2 and 3: In the text, you say uncertainty in w is ~88% and ~98% (which is probably low given that Kz is at least 100% and piston velocity is ~30%). Also, uncertainty in nutrient fluxes should be about the same. Why do these tables not show uncertainty as ~100%? I think they are now too low and misleading.
Tables 2 and 3 show the error of the mean value, which is the error from table 1 (88% and 98% respectively (68% and 100% in the revised version)), divided by the square root of the number of measurements from each region. Thus the error is smaller than 88% or 98%.
Tables: Where are the delta-3He values from below the mixed layer? Please show all measurements in a table somewhere.
Same answer as for 'Pg 26, Line 13':
For each profile, the depth range between 5 and 25 m below the mixed layer (at this profile) is used to calculate the helium-3 value of box 2. Reporting this depth for each profile would need to list more than 100 depth ranges, which we think is not practicable.

Figure 3: This relation is hard to see and I do not know if the fit is statistically significant. Please provide statistics with this plot if you are going to use this fit in the paper.
The fit is not used any more, and the figure is dropped.

Figure 5: I do not understand why you would adjust the 'red' He numbers for presence of surfactants if you do not show any evidence that surfactants are in fact present. It seems like an arbitrary adjustment of the data. The uncertainties are also not consistent with the text.
The uncertainties are the same as in table 1. Note that the error of the mean values presented here is smaller than the error of a single value by 1/sqrt(n), where n is the number of data points.
The largest discrepancy between coastal wind and helium derived vertical velocity is for the Peruvian region. That, and the observation of the wave damping by surfactants on cruise M91 (Kiefhaber et al., 2015) off Peru led to the decision to use a reduced gas transfer velocity in this case.

Figures 7 and 8: I don't see any relationship here. Also, please show uncertainty for these estimates.
Figure 7 has been removed.
We admit that the uncertainty is high, but do not know how to indicate the error bar at each data point without making the figure unreadable. The uncertainty is now mentioned in the legend.
Figure 8 has been modified, instead of WHe now the difference WHe – Wwind is shown.

Figure 9: Mauritania SSH anomaly looks very different for each cruise. Presumably, the SSH in Peru is also very different through time. I don't think this helps your case that eddies are such a large contributor to upwelled nutrient fluxes. Most likely, you need a time-weighted estimate through diurnal/weekly/monthly time frames to estimate the true NSS change.
We admit that a longer time series would allow to compute mean nutrient fluxes which are more representative for the regions. However, data from cruises only allows to compute quantities for the time of the cruise. Also the eddy field is changing with time, but the time scale for the eddies to influence the vertical velocity is in the order of days. We think it is appropriate to use the weekly mean eddy fields together with the vertical velocities from point measurements, which are also means over the period that is given by the gas exchange time scale.

Figure 11: This figure is difficult to interpret. I can't see the gray dots well. I'm not sure I see the point of displaying the data this way. The range of values is equal to the uncertainty... I suggest dropping this figure. Overall, I think there are too many figures.
The number of grey scales has been reduced to three to make them better distinguishable. Although the error of the pointwise data points is in the order of 100%, we think the pattern reflects the satellite distribution of productivity quite well. We followed the suggestion to reduce the number of figures and removed figure 10 instead. Overall, the paper now has three figures less.

Technical Corrections:
Pg. 20, Line 8: Please add the uncertainty to these values.
Done.

Pg. 23, Line 2: If you are only presenting PO4 and 3He, then why tell the reader about other measurements? This is unnecessary and should be removed.
We dropped the presentation of salinity measurements.

Pg. 26, Line 6: 'typically one or two data points per profile.' - They MUST be at least two if you are using a two-box model, right?
1-2 is the number of measurements within the mixed layer (see line 5), i.e. for box 1 alone.

Pg. 34, Line 7: If this boundary isn't the 500m isobath, then please show it on the map.
Done, instead of the region onshore of the 500 m isobath the 'coastal region' is now shaded grey.

Pg. 40, Line 27: Please add the uncertainty to these values in the text.
Done.
Table 1: For vertical mixing, "factor of 2" should read 100%. For winds, uncertainty should be ~30%. The resulting uncertainty should also be adjusted.
We recalculated the uncertainty for 30% error of the piston velocity (as mentioned above in this review). We think "factor of 2" is more appropriate than 100%, because for the error calculation we multiplied the diffusivity with "2" and divided it by"2".

Figure 1: Can you please add the uncertainty on the 3He measurements in the caption?

Done.

Figure 10: Can you please show the uncertainty? This should not be published without a clear statement at least that says these estimates are at least as uncertain as the upwelling estimates (you claim ± 100% in text).
This figure has been removed.

Manuscript prepared for Biogeosciences Discuss.
with version 2014/09/16 7.15 Copernicus papers of the LaTeX class copernicus.cls.
Date: 16 November 2015

Coastal upwelling off Peru and Mauritania inferred from helium isotope disequilibrium

R. Steinfeldt[1], J. Sültenfuß[1], M. Dengler[2], T. Fischer[2], and M. Rhein[1]

[1]Institute of Environmental Physics, University of Bremen, Bremen, Germany
[2]GEOMAR, Helmholtz Centre for Ocean Research, Kiel, Germany

Correspondence to: R. Steinfeldt (rsteinf@physik.uni-bremen.de)

Abstract

~~Oceanic upwelling velocities~~Upwelling is an important process, bringing gases and nutrients into the ocean mixed layer. The upwelling velocities, however, are too small to be measured directly. ~~The~~ Here we use the surface disequilibrium of the $^3He/^4He$ ratio ~~provides an indirect method to infer vertical velocities at the base of the mixed layer. Samples of helium isotopes were taken from~~ measured in two coastal upwelling regions ~~, off Peru on cruise M91,~~ off Peru in the Pacific ocean and off Mauritania ~~on 3 cruises. The helium-3 flux into the mixed layer also depends on the diapycnal mixing. Direct~~ in the Atlantic ocean to calculate the regional distribution of vertical velocities. To also account for the fluxes by diapycnal mixing, microstructure-based observations of the vertical diffusivity have been performed on all ~~4 cruises and are also used~~ four cruises analyzed in this study. The ~~resulting~~ upwelling velocities in the coastal regions vary between ~~1.1×10^{-5} and 2.8×10^{-5} m s^{-1}~~ $1.1 \pm 0.3 \times 10^{-5}$ and $2.8 \pm 1.5 \times 10^{-5}$ m s^{-1} for all cruises. Vertical velocities ~~off the equator can also be~~ are also inferred from the divergence of the wind driven Ekman transport. In the coastal regimes, ~~the agreement between wind and helium derived upwelling is fairly good at least for the mean values~~both methods agree within the error range. Further offshore, the helium derived ~~upwelling~~ vertical velocity still reaches 1×10^{-5} m s^{-1}, whereas the wind driven upwelling from Ekman suction is smaller by ~~at least~~ upto one order of magnitude. One reason for this difference ~~might be~~ is asrcibed to eddy induced upwelling. Both advective and diffusive nutrient fluxes into the mixed layer are calculated based on the helium derived vertical velocities and the ~~measured~~ vertical diffusivities. The advective part of these fluxes makes up at ~~least~~ about 50 % of the total. The nutrient flux into the mixed layer in the coastal upwelling regimes is equivalent to a net community production (NCP) of ~~1.3 g C m^2 d^{-1}~~ 1.3 ± 0.3 g C m^2 d^{-1} off Peru and ~~1.6–1.9~~ $1.6 - 2.1 \pm 0.5$ g C m^2 d^{-1} off Mauritania.

1 Introduction

Eastern boundary upwelling systems (EBUS), such as the Canary, California, Humboldt, and Benguela Currents belong to the most productive marine ecosystems , e. g. (Fréon et al., 2009). The upwelling is caused by the wind-driven surface circulation. Alongshore trade winds drive an offshore Ekman flux, which leads to a horizontal flow divergence at the coast and as a consequence upwelling of cold and nutrient-rich subsurface water. They also transport climate relevant trace gases such as N_2O from the ocean's interior into the mixed layer and ultimately into the atmosphere (Kock et al., 2012).

Crucial to quantify the role of upwelling for nutrient and tracer budgets is the vertical velocity, by which substances and gases are transferred from the subsurface into the mixed layer. ~~They are~~It is, however, much too small to be measured directly~~, but need to be inferred either from the divergence of the wind field or with the helium method, which has been established by Klein and Rhein (2004) and Rhein et al. (2010) . This method~~ . In previous studies upwelling has been derived from the wind field via Ekman theory (McClain, 1993; Hagen, 2001) , the divergence of the horizontal velocity fields inferred from current meters, drifters, and shipboard measurements (Weingartner and Weisberg, 1991; Gouriou and Riverdin, 1992) and geochemical tracers such as ^{14}C (Broecker et al., 1978; Quay et al., 1983; Toggweiler et al., 1991) , pCO_2 and AOU (Wanninkhof et al., 1995) , CFC-12 and SF_6 (Tanhua and Liu, 2015) as well as the isotopes ^{7}Be (Kadko and Johns, 2011; **?**) and ^{3}He (Klein and Rhein, 2004; Rhein et al., 2010) .

The helium method (Klein and Rhein, 2004; Rhein et al., 2010) exploits the excess of the helium isotope ^{3}He in the upwelled waters to determine the vertical velocity. The oceanic source for ^{3}He is hydrothermal venting, mainly near mid-ocean ridges, where primordial ^{3}He is emitted (Lupton, 1983). The ~~concentrations of ^{3}He originating from the release at mid ocean ridges are highest in the Pacific. From there, ^{3}He rich waters enter the Atlantic via the Antarctic Circumpolar Current, so in the Atlantic a north-south gradient of ^{3}He is established, with the waters of northern origin having a smaller helium-3 excess. The~~ ^{3}He

enriched waters eventually reach the mixed layer, e. g. by upwelling, where the excess ^{3}He is outgassing from the ocean. ~~Another approach akin to the helium method is based on Beryllium isotopes and was used by Kadko and Johns (2011) to infer vertical velocities in the tropical Atlantic. This method exploits the fact that the upwelled water is completely void of the isotope ^{7}Be.~~

Another process resulting in a net flux of properties from the ocean interior into the mixed layer is diapycnal mixing. Together with the helium measurements microstructure profiling has been performed at a large number of stations, and the diapycnal diffusivity has been inferred from the data off Mauritania (Schafstall et al., 2010). These authors found elevated dissipation rates of turbulent kinetic energy particularly at the continental slope close to the shelf break.

Here we investigate (i) the coastal region off Peru from 5 to 16° S that is part of the Humboldt Current upwelling system and (ii) the southern part of the Canary system off Mauritania between 20 and 16° N. Both, the Peruvian and the Mauritanian upwelling regions have in common that they are adjacent to oxygen minimum zones (Karstensen et al., 2008). This oxygen minimum is most pronounced in the Humboldt current south of 10° S, where denitrification within the upwelling water occurs. By this process also N_2O is produced, whereas in the Mauritanian upwelling the main production pathway for this substance is nitrification (Kock et al., 2012).

In contrast to the study of Rhein et al. (2010) at the equator, in the upwelling region off Peru and Mauritania the Ekman theory can be applied to infer the vertical velocity. ~~We will thus compare the Ekman and helium derived vertical velocities.~~ After presenting the data and methods, the Ekman and helium derived vertical velocities in the ~~coastal~~ upwelling regions are compared~~, and the role of vertical velocities related to eddies~~. Therefore, the cases for the open ocean (offshore region) and the case of a lateral boundary (for the coastal region) are considered. Also the role of eddies related to vertical velocities (eddy pumping) is investigated (McGillicuddy et al., 2007). Then the contribution of the upwelling and diapycnal mixing to the nutrient fluxes into the mixed layer are calculated.

2 Data

From the Peruvian upwelling area, about 300 helium samples have been taken at 62 stations during the cruise Meteor M91 in December 2012. In this region, upwelling occurs throughout the year, with medium offshore transport in boreal fall/early winter (Carr and Kearns, 2003). Helium measurements in the upwelling region west of Mauritania have been performed on three cruises (Fig. 1) The first cruise, M68/3 on RV *Meteor*, was conducted during boreal summer 2006 (July–August), but was mainly located north of 18° N. During the main upwelling season in boreal winter, two cruises with helium data are available: P347 with the German research vessel Poseidon took place in January 2007 and was restricted to the near coastal region, whereas on ATA3 (French vessel L'Aatalante, February 2008), a larger area was sampled but with less spatial resolution. Altogether, about 500 helium samples have been taken at 101 stations. All above mentioned cruises were part of the German research program "Surface Ocean Processes in the Anthropocene (SOPRAN)".

CTD$-O_2$ profiles were collected using a Seabird SBE 911 system attached to a carousel water sampler with 10 L Niskin bottles. Water ~~probes~~ subsamples from the Niskin bottles were used for the analysis of biogeochemical properties (nutrients, helium isotopes)~~as well as for the calibration of the Seabird conductivity sensor. The accuracy of the calibrated salinity data from the CTD is in general better than 0.003~~. From the biogeochemical parameters only PO_4 and helium isotopes are used in this study. The upwelling areas off Peru and off Mauritania are located within oxygen minimum zones (OMZ), and the low oxygen concentration due to the remineralisation of organic matter is correlated with high nutrient values. Off Peru, oxygen concentrations in the OMZ are so low that denitrification occurs at some places. Therefore we consider here only phosphate fluxes and not nitrate to avoid having to deal with the influence of the OMZ. On the four cruises, phosphate was measured with different autoanalyzers, the precision is about $0.02\,\mu mol\,kg^{-1}$.

The isotopes ^3He and ^4He were analyzed with the Bremen high-resolution static mass spectrometer (Sültenfuß et al., 2009). A very high resolution is necessary to distinguish

between the mass-3 hydrogen species $^1H^2H$ (HD) and ^3He. In this study, the isotopic ratio $^3He/^4He$ will be used as tracer for upwelled waters, which is expressed as $\delta^3He[\%]$, i. e. the relative deviation from the atmospheric ratio:

$$\delta^3He[\%] = \frac{\left(^3He/^4He\right)_{water} - \left(^3He/^4He\right)_{air}}{\left(^3He/^4He\right)_{air}} \cdot 100.$$

the measurement precision for the $^3He/^4He$ ratio is in general $\pm 0.4\,\%$ or better (Sültenfuß et al., 2009). This value is confirmed by the standard deviation of repeat samples taken mainly on cruises M91 and P347.

~~Figure~~Fig. 1 shows the locations and δ^3He in the mixed layer for the M91 cruise in the Peruvian upwelling region and the cruises M68/3, P347, and ATA3 off Mauritania. δ^3He values fall in different ranges for the two oceans. This is the result of the ~~aforementioned~~ difference of the helium-3 concentration in the subsurface waters of the ~~Pacific and the Atlantic~~two upwelling regions (see Fig.2). This difference can even be seen in the mixed layer, thus indicating the entrainment of water into the mixed layer from below.

In order to distinguish between advective and diffusive vertical ^3He fluxes into the mixed layer, knowledge of the diapycnal diffusivity is an important factor. This quantity is determined from microstructure shear data that were collected on all cruises using different tethered microstructure profilers (MSS90L and MSS90D). Both instrument types are equipped with two airfoil shear sensors, a fast temperature sensor (FP07), an acceleration sensor, tilt sensors, and standard CTD sensors. For a detailed description see Prandke and Stips (1998). From the small scale velocity fluctuations measured by the MSS instruments, dissipation rates of turbulent kinetic energy ϵ are derived by integrating shear wavenumber spectra assuming isotropic turbulence. Processing details are described in Schafstall et al. (2010), where the microstructure shear data from the Mauritanian area are presented. After applying corrections for unresolved spectral ranges and loss of variance due to the finite sensor tip finally the diapycnal diffusivity K_ρ is inferred via the Osborn (Osborn, 1980) rela-

tionship:

$$K_\rho = \Gamma \frac{\epsilon}{N^2}.$$

N denotes the local buoyancy frequency, and Γ the mixing efficiency, which is set to a constant value of 0.2 (Oakey, 1982).

In addition, remote sensing data of wind speed, primary production and sea surface height are used in this study. These data are available via internet. The wind speed U_{10} is taken from the daily gridded ASCAT (ftp://ftp.ifremer.fr/ifremer/cersat/products/gridded/mwf-ascat/data/daily) wind product (for cruiuse M91 in 2012) and the older QuikSCAT product (ftp://ftp.ifremer.fr/ifremer/cersat/products/gridded/mwf-quikscat/winds/daily, for the Mauritanian cruises in 2006–2008). For primary productivity, the 8 day MODIS based estimates from http://www.science.oregonstate.edu/ocean.productivity/index.php were used. The algorithm for computing primary production is based on Behrenfeld and Falkoweski (1997). Also used in this study are sea level anomalies from the Aviso product (http://www.aviso.oceanobs.com/duacs/).

3 Methods

In order to compute the upwelling velocity from the ^{3}He disequilibrium, the same box model as in Rhein et al. (2010) and Klein and Rhein (2004) is applied. This model only has a vertical dimension with two boxes. The upper box 1 represents the mixed layer, ~~and the~~ where gas exchange with the atmosphere takes place. The lower box 2 exchanges properties with box 1 by advective and diffusive vertical fluxes. This box thus supplies the upwelling ~~of~~ water enriched in ^{3}He. ~~It is assumed that the $^3He/^4He$ ratios in both boxes remain constant along the pathway of the patch of surface water, at least for the equilibration time scale given by the helium gas exchange (4–8). This implies that~~ In steady state, the upward advective and diffusive ~~flux~~ fluxes of ^{3}He from box 2 into the mixed layer

~~is compensating~~ (box 1) are compensated by outgassing of ^{3}He from box 1 into the atmosphere. This steady state assumption results in the following equation for inferring the vertical velocity w:

$$\frac{DC_1}{Dt} = 0 = F_\mathrm{g} - K_\mathrm{v}\frac{\mathrm{d}C}{\mathrm{d}z} + w(C_2 - C_1). \quad (1)$$

The same 1-D box model has been used in (Tanhua and Liu, 2015) for CFC-12 and SF_6. Kadko and Johns (2011) and Haskell et al. (2015) use a modified version for the inventory of ^{7}Be. All these models neglect horizontal advection, i. e it is assumed that changes of the respective tracer in the mixed layer is dominated by vertical processes. Another interpretation is that Eq. 1 is valid in a Lagrangian coordinate system moving with the surface patch (box 1), as long as the lower box 2 moves with a similar velocity and horizontal mixing is small.

Applying the box model, the values of the gas exchange rate F_g, the vertical diffusivity K_v (which is assumed to be equal to the diapycnal diffusivity K_ρ) and the vertical δ^3He gradient below the mixed layer $\mathrm{d}C/\mathrm{d}z$ and the δ^3He ratio C_1 and C_2 in boxes 1 and 2, have to be determined for each profile. We mainly follow the procedure in Rhein et al. (2010), but with some differences in detail.

The gas exchange rate

$$F_\mathrm{g} = v_\mathrm{g}\Delta C, \quad (2)$$

is given by the gas transfer velocity v_g and the helium-3 disequilibrium in the mixed layer $\Delta C = C_\mathrm{eq} - C_1$. The equilibrium δ^3He ratio C_eq is $-1.6\,\%$. The gas transfer velocity v_g has been calculated using the relationship given by Nightingale et al. (2000):

$$v_\mathrm{g} = 0.01/3600 \cdot (0.222\,U_{10}^2 + 0.333\,U_{10}^3) \cdot (\mathrm{Sc}/600)^{-0.5} \quad (3)$$

The gridded wind speed U_{10} is interpolated on the locations of the helium measurements, and the daily values are averaged over a time period of n days in advance of the sampling

date. n depends on the time scale of the gas exchange, i. e. the mixed layer depth and the gas transfer velocity itself. n has been calculated as mean value for each cruise and varies between 4 (cruise M68/3) and 8 (cruise P347) days.

The mixed layer value C_1 for δ^3He (also for nutrients) is calculated as the mean of all measurements within the mixed layer at each station. For bottle data as helium and nutrients, these are typically one or two data points per profile. The mixed layer depth is determined according to Levitus (1982) with a density threshold of $\Delta\sigma\theta = 0.125\,\mathrm{kg\,m^{-3}}$. In addition, a visual examination of each profile has been applied to avoid an erroneous allocation of bottle data to the mixed layer. This could be caused by the fact that the mixed layer depth is determined from CTD data during the downcast, whereas the Niskin bottles are closed during the upcast.

In order to estimate the δ^3He ratio of box 2 C_2, the vertical mean values of δ^3He for each profile are computed over an interval 5 and 25 m below the mixed layer. The relatively sparse bottle data (helium and nutrients) are vertically interpolated onto 1 m intervals using a piecewise cubic Hermite polynomial interpolation scheme that preserves the shape of the data as in Tanhua et al. (2010), and then the vertical mean value is calculated. The depth range from 5 to 25 m below the mixed layer is much smaller than in Rhein et al. (2010), but comparable to those used in Tanhua and Liu (2015) applying the same box model and in Schafstall et al. (2010) and Kock et al. (2012) for calculating diffusive fluxes of nitrate and N_2O into the mixed layer. Directly at the base of the mixed layer, vertical mixing might dominate (Kadko and Johns, 2011), but the large concentration gradient of ^{3}He (and also nutrients) cannot be resolved by the coarse resolution of the bottle data. We thus determine the diffusive and advective helium-3 flux from the data in box 2 and assume that these fluxes are continuous into the mixed layer, i. e. no flux divergence or convergence occurs in the "gap" of 5 m between the boxes 1 and 2. In Rhein et al. (2010), C_2 was calculated as regional mean over several profiles. This is not done here, as the regions adjacent to the coast shows a large variability in C_2 (see Fig. 2g and h), so the original values for each helium-3 profile are retained.

Turbulent fluxes of ^{3}He into the mixed layer are estimated from the diffusion coefficient based on the microstructure shear data and the vertical δ^3He gradient. Both K_v and $\mathrm{d}C/\mathrm{d}z$ in Eq. (1) are averaged over the same range 5–25 m below the mixed layer as the ^{3}He values for calculating C_2. At some profiles, only helium, but no microstructure data are available. ~~The diapycnal diffusion is typically increasing towards the shelf, e.g. the continental slope off Mauritania acts as a mixing hot spot (Schafstall et al., 2010) . Thus for the helium profiles whitout microstructure data the vertical diffusion is derived from a linear relation between diffusivity and the logarithm of the water depth, which has been derived from all available microstructure profiles (Fig. 3). The mean deviation of the fitted values from the original vertical diffusivities is about 30 %~~In these cases, the regional mean value of K_v over coastal and offshore rgeions respectively has been used.

4 Property distribution in the coastal upwelling areas

The distribution of temperature, phosphate and helium-3 is shown in Fig. 2 for a section along 8° S in the Peruvian upwelling, the long 18° N section off Mauritania from cruise M68/3 and a short section also along 18° N from cruise P347. The ideal case of coastal upwelling is represented by the section off Peru (Fig. 2, left column): the isolines of all properties and also the isopycnal charecterizing the central water ($\sigma_\theta = 26.0\,\mathrm{kg\,m^{-3}}$) are lifted up towards the coast due to upwelling, and the mixed layer becomes shallower. A similar general feature can be observed along the 18° N section for the cruise P347 (Fig. 2, right column), at least for the upper 50 m of the section and the isopycnal $\sigma_\theta = 26.0\,\mathrm{kg\,m^{-3}}$. Near the coast below ≈ 50 m depth, the isolines are declining downward towards the coast for both cruises from the ~~Maritanian upwelling. This might be the consequence of the enhanced diapycnal mixing over the shelf break. Another reason could be the northward surface velocity in that area observed from shipboard acoustic doppler current profiler measurements (Schafstall, 2010) . This current direction is opposite to the geostrophic flow that would be expected for coastal upwelling(equatorward due to an offshore increase in sea surface height). Assuming thermal wind balance, isopycnals sloping downward towards~~

~~the coast would lead to a reduction of the northward surface flow with depth.~~ Mauritanian upwelling.

The 18° N section of cruise M68/3 (Fig. 2, middle column) has the largest ~~offsore~~ offshore extension of all sections from the two upwelling regions. The isolines and also the bottom of the mixed layer show a ~~conspicious~~ conspicuous uplift towards the east between 24 and 20° W. This is the location of the Canary Current advecting water from the upwelling systen further north, which can be seen from the relatively low water temperature in the mixed layer. The water within the coastal upwelling region is fed from the south by South Atlantic Central Water (SACW) (Hagen, 2001) and is more enriched in nutrients and helium-3 and less saline (i. e. colder along isopycnals) than the North Atlantic Central Water, which can be found west of the Canary Current in the interior of the northern subtropical gyre. The Central Water off Peru is clearly more enriched in phosphate and helium-3 than off Mauritania.

~~The temperature in the upwelling region is coldest off Peru and only slightly warmer for the winter cruise P347 off Mauritania, reaching from 13–15 at 150 to 16–20 at the surface. The summer cruise M68/3 from the Mauritanian area shows much higher temperatures towards the surface, up to 27 due to seasonal warming. The advection of colder water with the Canary Current from the north between 24 and 20 W and of warm water from the south in the coastal area has a large influence on the sea surface temperature.~~ In all three sections, δ^3He values in the mixed layer are in general larger than the equilibrium of $-1.6\,\%$. This is especially so in the Pacific due to the high helium-3 content of the upwelled waters. Offshore in the Atlantic, on some locations, equilibrium values are found, for instance west of 24° W during cruise M68/3 (Fig. 2h).

The lowest row in Fig. 2 shows the δ^3He values of box 1 (C_1) (the mixed layer) and box 2 (C_2) (5–25 m below the mixed layer), which are used in Eq. (1) to infer the upwelling velocities. For the 8° S section of cruise M91 off Peru, both (C_1) and (C_2) are increasing landward, as would be expected for enhanced upwelling at the coast. The difference between (C_1) and (C_2) decreases in onshore direction from about 2 to 1 % in δ^3He, indicating an enhanced exchange between both layers by upwelling and/or diapycnal mixing. In the western subtropical gyre area of the 18° N of cruise M68/3, the δ^3He values in box 1 and

2 are almost identical, as the NACW is depleted in helium-3. Further east, where SACW is dominating below the mixed layer, the difference between (C_1) and (C_2) is larger but decreases towards the coast, as for the section off Peru. Also for the much shorter 18° N section of cruise P347 the upwelling and/or mixing near the coast lead to a relatively small difference between the δ^3He values in box 1 and 2. The almost identical values of (C_1) and (C_2) at 17° W might result from a data gap below the mixed layer (see the location of helium samples in Fig. 2i). Note that some stations along this line have been repeated within a few days, so for some locations two mean values in box 1 and box 2 exist. For the Mauritanian upwelling, δ^3He within box 1 reaches the equilibrium value of $-1.6\,\%$ at about 17° W for both cruises. However, during M68/3 further west at some stations an oversaturated mixed layer concentration of helium-3 has been observed, indicating upwelling also at those offshore locations.

5 Results and discussion

5.1 Helium derived upwelling velocities

The upwelling velocities calculated according to Eq. (1) are shown in Fig. ~~4~~ 3 for all four cruises. Negative values of w are set to zero, so possible downwelling is not considered here. Small differences $C_1 - C_2$ in the denominator of Eq. (1) result in large upwelling velocities. In order to guarantee that such high vertical velocities are not the consequence of uncertainties in the helium measurement, values for w from Eq. (1) are discarded if the absolute value $|C_1 - C_2|$ is smaller than the quadratic sum of the uncertainties of C_1 and C_2, both numbers are assumed to be 0.2 % in δ^3He units (see next subsection and Table 1).

Overall, at about 60 % of the stations with δ^3He measurements in the mixed layer upwelling occurs (~~28~~ 26 out of 49 stations for M91 and ~~47~~ 43 out of 74 for the Mauritanian cruises). The resulting vertical velocities are of the order of $10^{-5}\,\mathrm{m\,s^{-1}}$ both for the Peruvian and for the Mauritanian regions.

Off Peru, regions of strong coastal upwelling are found in the northern area between 5 and 8° S. ~~Here, no decrease in offshore direction of the upwelling velocity can be observed.~~ Another region with ~~strong upwelling further south~~ high vertical velocities further south at 12–14° S is restricted to the coast~~, further offshore~~. Around 10° S and south of 15° S the upwelling is weak or even vanishing.

The three cruises off Mauritania have a different regional extension. Cruise P347 is restricted to the coast, but with a very dense station spacing. The maximum of the upwelling is located south of 18° N near the coast onshore of the 500 m isobath. The other two cruises which cover a larger area (M68/3 and ATA3) show that the upwelling near the coasts persists up to 20° N near Cape Blanc. For these cruises, also at some locations west of 18° W enhanced upwelling is observed. Combining the results from the three cruises from the Mauritanian region, the whole picture is that in offshore direction the vertical velocity first decreases and then increases again at some locations.

5.1.1 Error estimation

The total error of the upwelling velocities is computed from the error of the single terms in Eq. (1). This comprises the helium values in boxes 1 and 2, C_1, C_2, the gas exchange and the vertical mixing. The $^3He/^4He$ ratio measured at the Bremen high-resolution mass spectrometer has a precision better than 0.4 %. The standard deviation of duplicate samples of the cruises presented here is even smaller, about 0.3 %. This error of the $^3He/^4He$ ratio is directly linked to the uncertainty of C_1, the $^3He/^4He$ ratio in the mixed layer. The number n_1 of samples from the mixed layer for a single profile, where C_1 is derived from, varies between 1 and 3. So the uncertainty of C_1 is $0.3\%/\sqrt{n_1} \approx 0.2\%$.

Below the mixed layer, again 1–3 helium measurements leave its mark for the calculation of C_2. Thus, the error of C_2 is also about 0.2 %.

~~As noted above, the diffusion coefficient K_v varies with depth .~~ Another topic is the depth range that is chosen for the calculation of C_2. The concentration of ^3He is typically increasing with depth, so a deeper depth range for calculating C_2 would lead to smaller upwelling velocities. This effect is partially compensated by the diffusive

term, as vertical mixing below the mixed layer often decreases with depth, but in most cases the effect of a depth increase of C_2 will dominate. This is in agreement with Kadko and Johns (2011) , who postulate a decrease of the upwelling velocity with depth. As noted in Tanhua and Liu (2015) , the upwelling velocities are valid only for the depth where C_2 is calculated, which is $5-25\,\mathrm{m}$ below the mixed layer in our case.

The relative standard deviations of K_v for deep and shallow regions is about 100 %. Compared to this large value, the error of the vertical helium-3 gradient can be neglected, so the vertical mixing is estimated to vary by a factor of 2 from the calculated value.

~~The gas exchangeis based on the mean daily~~ For the gas exchange, an error of 30 % for the piston velocity is assumed. This error comprises both variations in wind speed over ~~a period of 4–8, depending on the cruise~~ the equilibrium time scale for the gas exchange (see above) ~~. The standard deviation of these mean wind speeds are of the order of 10 % and are computed for each profile separately. As the gas transfer velocity v_g is a quadratic function of the wind speed, the resulting error of v_g is larger than 10 %. Uncertainties~~ and errors in the parameterization of the ~~gas transfer velocityare neglected~~piston velocity. All these errors are listed in Table 1.

The influence of the errors of the input values on the upwelling velocity w is non-linear (see Eq. 1). Thus the upwelling velocities are calculated for adding and subtracting the errors from the input values. In this way, a minimum and a maximum upwelling velocity is computed, and the error is assumed to be half of the difference. This is done for each source of error separately. In the Peruvian upwelling, both surface as well as subsurface helium-3 concentrations are much higher than off Mauritania (Figs. 1 and 2). Thus, the “signal to noise ratio” of C_1 and C_2 and the is larger for the ~~Peruvian upwelling~~region off Peru, and the error estimation is done separately for both upwelling regions.

The relative errors of w for each source of error are shown in Table 1. Although the uncertainty of C_1 and C_2 is the same, the resulting error in the upwelling velocity w is much larger for C_1 than for C_2. This is because C_1 appears in Eq. (1) not only in the nominator (C_1-C_2), but also influences the magnitude of the gas exchange in the nominator of Eq. (1). A change of C_1 in one direction causes a change of w in the same direction for both terms.

As was expected, the better signal to noise ratio of C_1 and C_2 for the Peruvian area results in a smaller error for w compared to the Mauritanian region. ~~The~~ Also the uncertainty of w resulting from the diapycnal mixing ~~is similar for both regions, whereas the error of the wind speed has a larger influence off Peru~~and the piston velocity is smaller for the Peruvian region. Note that the ~~observed wind speeds there during cruise M91 (about 4 m s^{-1}) are smaller than for the cruises off Mauritania (5–8)~~uncertainty of w due to vertical mixing is much smaller than the error of the mixing itself, as in many cases the term for the vertical diffusion in Eq. 1 is small compared to the gas exchange term. The total error ~~of w is~~ calculated as the quadratic sum of the four ~~errors from the input data and adds up to 81 % for the M91 data and 98 % for the three cruises~~ error terms of the inferred upwelling velocity is 68 % off Peru and 100 % off Mauritania.

5.2 Comparison between helium and wind derived upwelling

We will now compare the upwelling velocities derived from the helium method (w_{Helium}) with those calculated directly from the wind field (w_{Wind}). In the open ocean away from coastal boundaries, the upwelling velocity at the base of the Ekman layer can be computed directly from the wind stress curl (see e.g. Gill, 1982):

$$w = \frac{1}{\rho}\left(\frac{\partial}{\partial x}\left(\frac{\tau_y}{f}\right) - \frac{\partial}{\partial y}\left(\frac{\tau_x}{f}\right)\right), \tag{4}$$

with water density ρ, Coriolis parameter f and the zonal and meridional components of the wind stress τ_x and τ_y. Near the coast, the lateral boundary is taken into account using a two-layer model (Yoshida, 1955). The solutions for the velocity u in the upper layer directed offshore and the vertical velocity w have the form (Gill, 1982):

$$u = -\frac{\tau_y}{\rho f H_1}(1 - e^{-x/a}) \tag{5}$$

$$w = \frac{\tau_y}{\rho f a} e^{-x/a}. \tag{6}$$

H_1 is the depth of the upper layer (Ekman layer), and τ_y denotes the wind stress component parallel to the coast. The spatial scale of the upwelling area is given by the first internal Rossby radius a. a is calculated for a two layer ocean with densities ρ_1 and ρ_2. ρ_1 is the density of the mixed layer. For ρ_2 we have chosen the mean density between the lower boundary of the mixed layer and 500 m depth, which is approximately the lower boundary of the central water from which the upwelled water originates. For each of the three cruises, a mean value of a is calculated, as the stratification and thus the Rossby radius between the cruises might differ. The resulting values are $a = 15$ km for M91, $a = 16$ km for M68/3, $a = 10$ km for P347 and $a = 12$ km for ATA3. The magnitude of the wind driven coastal upwelling velocities at each station depends on the choice of the Rossby radius a in Eq. (6). The total vertical transport integrated over the coastal area, ~~however, is~~ i. e. a distance of several Rossby radii, is almost independent from a. The alongshore velocity (coastal jet) in Eq. (5) increases linearly with time~~i. e.~~, so this solution does not represent a steady state. More complex solutions can be found (Fennel, 1999) where the increase of the coastal jet is limited due to the generation of coastal trapped Kelvin waves.

x in Eqs. (5) and (6) denotes the distance from the coast. The continental shelf in the study area is relatively broad, and the mixed layer in this region has a mean depth of 10–25 m. The upwelled water has to be supplied from below the mixed layer, but this is only possible if the water depth is considerable larger than the mixed layer (more correct: Ekman layer) depth itself. We thus assume a minimum water depth of 50 m (two times the mixed layer depth) for wind driven upwelling to occur and set x as the distance from the 50 m isobath. In this case, w_{Wind} calculated according to Eq. (6) is comparable in magnitude with w_{Helium} (Fig. ~~5a~~4a). Setting $x = 0$ directly at the coast leads to w_{Wind} being one order of magnitude smaller. As wind driven vertical velocity w_{wind} which has to be compared with w_{Helium} we choose the maximum value of both calculations according to Eqs. (4) and (6), which means that either the influence of the coastal boundary is dominating the vertical Ekman velocity or the wind stress curl over the open ocean.

w_{Wind} is calculated from the gridded daily wind data which are interpolated onto the station locations in the same way as for calculating the gas exchange velocity. Also for

w_{Wind} the temporal mean over the period that is given by the gas exchange time scale (n days, see Sect. 3) is taken. So w_{Wind} covers the same time scale of n days as w_{Helium}. Nevertheless, there is a difference in the interpretation of the temporal mean of w_{Wind} and w_{Helium}. Whereas w_{Helium} has to be interpreted as the Lagrangian mean following the patch of surface water, w_{Wind} is the Eulerian mean. Another difference between w_{Wind} and w_{Helium} is the fact that w_{Helium} strictly speaking describes the entrainment velocity: $w_{\text{Helium}} = w_{\text{Wind}} - \partial z_{\text{mld}}/\partial t$. Here, z_{mld} denotes the lower boundary of the mixed layer.

To overcome the difference between these methodological differences and also to reduce the large error of the pointwise w_{Helium} data, regional mean values of w_{Wind} and w_{Helium} are calculated. For these mean values, the differences between Eulerain and Lagrangian mean as well as between vertical and entrainment velocity should be reduced. The regions are the area within the 50 km distance to the 50 m isobath, where the boundary solution from Eq. (6) is typically larger than the open ocean result from Eq. (4), all stations with larger distance from the coast make up the other region. These areas will be referred to as "coastal", and "offshore" respectively. The ~~boundary between both regions is often located close to the 500isobath, i.e. the grey shaded area in Figs. 1 and 4 is almost identical with the "coastal" region. The~~ error of the regional mean values of w_{Wind} and w_{Helium} is ~~simply the~~ the standard deviation of the ~~vertical velocity at all stations~~ pointwise velocity data within the region with helium data divided by the ~~squareroot~~ square-root of the number of those stations. For the helium derived upwelling, this error is typically larger than dividing the 100 % error of the single measurements by the square root of the number of data points. The reason is that vertical velocities in one region arevarying by upto an order of magnitude.

All mean values for the coastal and offshore regions for each cruise are given in Table 2 and represented graphically in Fig. ~~5.~~ 4. For the coastal regions, mean upwelling velocities are of the order of $10^{-5}\,\mathrm{m\,s^{-1}}$, whereas for the offshore regions they vary between $10^{-5}\,\mathrm{m\,s^{-1}}$ and only $10^{-6}\,\mathrm{m\,s^{-1}}$. The coastal values for w_{Helium} and w_{Wind} off Mauritania agree for all three cruises within their error bars. The winter cruise P347 shows the smallest coastal upwelling ~~$1.4 \times 10^{-5}\,\mathrm{m\,s^{-1}}$, whereas the~~ $1.4 \pm 0.4 \times 10^{-5}\,\mathrm{m\,s^{-1}}$. The other winter cruise ATA3 and also the summer cruise M68/3 have ~~significantly~~

~~larger values 2.1×10^{-5}~~larger values $2.1 \pm 0.8 \times 10^{-5}$ ~~$2.8 \times 10^{-5}\,\mathrm{m\,s^{-1}}$~~$2.4 \pm \times 10^{-5}\,\mathrm{m\,s^{-1}}$. These numbers, however, agree within their error bars. This implies that no seasonal variation of the upwelling has been observed, but the limited number of three cruises ~~mihgt~~ might not be representative for the ~~seasonal mean~~respective season. Offshore, only for cruise P347 w_{Helium} is small ($0.2 \times 10^{-5}\,\mathrm{m\,s^{-1}}$). For all Mauritanian cruises w_{Helium} surpasses w_{Wind} ~~by one order of magnitude~~ in the offshore region.

For the Peruvian area, the differences between w_{Helium} and w_{Wind} show an opposite behaviour: they are relatively small for the offshore region, but large for the coastal area ($\approx 1.1 \times 10^{-5}\,\mathrm{m\,s^{-1}}$ for w_{Wind} in contrast to $\approx 2.7 \times 10^{-5}\,\mathrm{m\,s^{-1}}$ for w_{Helium}). One reason for the high value of w_{Helium} might be an overestimation of the gas exchange velocity in Eq. (3) due to the presence of organic surface films (~~surfactant~~surfactants). These films have been observed on cruise M91, and their damping behaviour on surface waves have been shown in Kiefhaber at al. (2015) . There, the observed mean square slope of the waves was found to be overestimated by the parameterization for clean water. Most measurements are in the range spanned by clean water and slick parameterizations. Surfactants also drastically reduce the transport of gases across the water surface. A parameterization of the gas transfer velocity in the presence of surfactant is given in Tsai and Liu (2003). However, there the gas transfer for the case with and without surface films are based on the parameterization form Liss and Merlivat (1986). For low wind speeds as have been prevailing during cruise M91, this formula results in smaller gas transfer velocities than Eq. (3) even for the normal case without surfactants. Including the reduction factor r from Tsai and Liu (2003) ($r = 0.56\,U_{10}^{-0.13}$) for the case with surfactant, the resulting gas exchange and thus the helium derived vertical velocities would almost vanish. We thus adopt the reduction factor from Tsai and Liu (2003), but apply it to the gas transfer velocity from Nightingale et al. (2000), Eq. (3). The resulting mean upwelling velocity for the coastal area is also given in Table 2 and Fig. ~~5a~~ 4a and in good agreement with the wind derived value w_{Wind}. ~~Figure 6~~ Fig. 5 shows the distribution w_{Helium} for the case of the reduced gas transfer velocity. Comparison with Fig. ~~4a~~ 3a for the standard gas exchange shows that the overall pattern of the distribution of the vertical velocities remains unchanged, only the coastal values are smaller.

In Kiefhaber at al. (2015) not all data points are influenced by surfactants. As illustrated in Fig 4a, the helium derived upwelling velocity based on reduced gas exchange at all coastal stations is slightly smaller than the wind derived one, indicating that the effect of surfactants is overestimated when being applied to all stations.

One could argue that the enhanced δ^3He values in the offshore region are the remnants from helium-3 rich water originating in the coastal upwelling and then have being advected offshore. Taking into account the equilibrium time scale for the helium gas exchange, after about 20 days the mixed layer disequilibrium of helium-3 should have decreased to about 10 % of the value from the upwelled water (< 0.1 % for the Mauritanian and < 0.2 % for the Peruvian upwelling), . Assuming an advection velocity of $\approx 10\,\mathrm{cm\,s^{-1}}$ in offshore direction, the water could move about 200 km away from the coast over the 20 day time period. For the Peruvian area, most stations are within this distance, so an influence from the coastal upwelling on the offshore helium-3 values cannot be excluded. For the Mauritanian region, enhanced δ^3He values can be found even west of 18° W, too far west to be remnants from the coastal upwelling. Possible explanations for the large offshore vertical velocities will be given below.

~~The comparison between the stationwise values of ω_{wind} and ω_{Helium} for all cruises is shown in Fig. 7. Filled and open circles represent the coastal and offshore regions respectively. Due to the above mentioned differences between wind (Eulerian, absolute velocity) and helium (Lagrangian, entrainmanet velocity) derived vertical velocities and the large error of the stationwise values discrepancies occur. As for the mean values, the larger helium derived upwelling in the Mauritanian offshore area is evident. For the coastal area off Peru, the ω_{Helium} values for the case of reduced gas exchange due to surfactant are shown. Despite of the large differences between the stationwise values of ω_{wind} and ω_{Helium} in some cases positive significant correlations between them exist. These are the cases using all data from M91 and P347, the offshore data from M91 and the coastal data from P347. All the mentioned correlations are in the range between 0.43 and 0.55 and significant on the 99 % levels.~~

5.3 Other upwelling mechanisms

The ~~large~~ discrepancies between the ~~pointwise~~ wind and helium derived upwelling velocities ~~,~~ especially in the offshore region ~~,~~ suggest the existence of additional upwelling mechanisms. These would be included in the helium derived vertical velocities, but not in the purely wind driven ones. For the region at the Mauritanian coast, large helium derived velocities for cruises M68/3 and ATA3 are located south of Cape Blanc near 20° N (Fig. ~~4b~~ 3b and d). These maxima do not show corresponding high values in the wind driven upwelling. Mazzini and Barth (2013) concluded from a model study that flow–topography interaction is upwelling favorable downstream of capes, a situation which is given south of Cape Blanc following the south westward direction of the Canary Current. Thus in this case the wind derived vertical velocity might be an underestimation.

A possible mechanisms explaining the high vertical velocities from the helium method which surpass the Ekman derived values by up to one order of magnitude is eddy induced upwelling. Several mechanisms for this phenomenon are possible: uplift of isopycnals close to the mixed layer, as they occur in cyclones and mode water eddies. Stramma et al. (2013) observed subsurface chlorophyll maxima in such typed of eddies in the Peruvian upwelling on cruise M90, just one month prior to the cruise M91 discussed here, and ascribed them to this mechanism. The helium method is however not able to catch this process as long as the uplifting of isopycnals does not lead to an intrusion of subsurface water into the mixed layer. In the opposite direction, when the upwelled water leaves the coastal area, the mixed layer might deepen, leaving to entrainment of water from below. This process would be classified as upwelling by the helium method. However, no correlation between enhanced offshore upwelling and deep mixed layers can be found from the data off Mauritania.

Ekman suction due to wind stress on the eddy is also suggested to foster upwelling (Martin and Richards, 2001). Here, at the side of the eddy where the eddy flow is in the same direction as the wind, the wind stress is reduced, whereas it is enhanced on the opposite side of the eddy, where wind and eddy flow are in the opposite direction. This difference in wind stress between both sides of the eddy induce an upwelling for anticy-

clones and mode water eddies and a downwelling for cyclones. Another mechanisms also desribed in Martin and Richards (2001) is upwelling by ageostrophic circulation resulting from a perturbation of the eddy flow field.

In order to investigate a possible influence of eddies on the helium derived upwelling velocity, the gridded AVISO sea level anomaly (SLA) has been interpolated on the station location. ~~Figure 8~~ Fig. 6 shows the interpolated SLA against ~~vertical velocity. the spatial distribution of SLA and~~ w_{Helium} ~~is shown in Fig. 9 fore each cruise. Whereas in Fig. 8 weekly means are used for SLA, in Fig. 9 the mean from the weekly SLA over the duration of the cruises is shown in order to get only one map per cruise and thus a comprehensive picture. From Fig. 8 it can be seen that upwelling occurs both for cyclones (negative SLA) and anticyclones~~$\Delta w = w_{\text{Helium}} - w_{\text{Wind}}$, i.e. the portion of the vertical velocity, which is not explained by wind driven upwelling. For the coastal data, no relation between SLA and Δw can be found. For the offshore data, towards the center of anticyclones (SLA $> 5\,\text{cm}$), the upwelling is slightly reduced. At offshore points with smaller SLA ($5\,\text{cm} > \text{SLA} > -5\,\text{cm}$), Δw is either positive or close to zero. If the two data points with $w_{\text{Helium}} > 4 \times 10^{-5}\,\text{m s}^{-1}$ are regarded as outliers, the offshore data form a triangular pattern with the edges at [-4cm/~~mode water eddies (positive SLA).~~ $0,\text{m s}^{-1}$], [$1\,\text{cm}/3 \times 10^{-5}\,\text{m s}^{-1}$] and [$5\text{cm}/0,\text{m s}^{-1}$].

The eddy–wind interaction can thus be ruled out as mechanisms responsible for the upwelling, as this only works for positive SLA. Another reason is that even in that case, for the moderate wind speeds observed during all cruises ($u_{10} < 10\,\text{m s}^{-1}$), the resulting upwelling would only be of the order of $10^{-6}\,\text{m s}^{-1}$. A strong upwelling of order $10^{-5}\,\text{m s}^{-1}$ as observed by McGillicuddy et al. (2007) only occurs for high windspeeds ($u_{10} > 10\,\text{m s}^{-1}$). ~~Figure 8 also shows that high vertical velocities only occur for moderate SLAanomalies of ± 5cm, i. e. at the edge of the eddies. In the center of the eddies at the extreme SLA values upwelling is appears to be suppressed. The maps in~~

The spatial distribution of SLA and Δw at the offshore data points is shown in Fig. 7 fore each cruise. Whereas in Fig. 6 weekly means are used for SLA, in Fig. 7 the mean from the weekly SLA over the duration of the cruises is shown in order to get only one map per

cruise and thus a comprehensive picture. Fig. ~~9. also support this view. We thus conclude that the ageostrophic instabilities~~ 7. illustrates that enhanced upwelling occurs at the edge of eddies at locations of small SLA. These enhanced verticval velocities are, however, not a general feature of eddy boundaries. We conclude that ageostrophic instabilities that might occur at the edge of eddies are the main mechanism for eddy induced upwelling. On the other hand, towards the center of anticyclones upwelling is weakened.

5.4 Nutrient fluxes

The coastal regions off Peru and Mauritania belong to the most productive areas of the world ocean. We thus consider the relation between nutrient supply into the mixed layer from vertical transports (both advective and diffusive) and net primary production (NPP) observed from ~~satllites~~ satellites (http://www.science.oregonstate.edu.ocean.productivity/index.php). The advective and diffusive phosphate fluxes into the mixed layer are computed in the same way as the helium-3 flux: the concentration of phosphate in box 2 (C_2), the phosphate gradient and the vertical diffusivity are calculated as vertical mean over the depth range 5–25 m below the mixed layer. If no microstructure data are available, the diffusion coefficient is ~~calculated from the logarithm of the water depth~~ set to the regional mean (see Sect. 3). As advective velocities in the Peruvian upwelling w_{Helium} derived from the reduced gas exchange is used, these values are in better agreement with w_{Wind}.

Similar to the SLA data, the 8 day mean values of satellite derived productivity are interpolated on the station locations. In order to allow for a reaction of the productivity to changes in nutrient supply, the productivity data are shifted in time by half a week. For a quantitative comparison between NPP and phosphate fluxes, the latter are converted to carbon units by multiplying with the Redfield ratio of 117 from Anderson and Sarmiento (1994). ~~Figure 10 shows these fluxes into the mixed layer against satellite observed NPP for all cruises. The only case where a significant correlation exists is for the offshore area of cruise M68/3. For all other cruises/regions, a large range of NPP is observed for similar carbon fluxes into the mixed layer.~~

The spatial distribution of NPP and vertical carbon transport is shown in Fig. ~~11~~ 8 for each cruise. As for SLA, the NPP values over the time period of each cruise are averaged to get one comprehensive map per cruise. Here, at least a qualitative correlation between NPP and carbon flux can be observed. At the northern end of the Peruvian area, e. g., enhanced carbon fluxes reach from the onshore up to the offshore end of the sections, and the area with enhanced NPP also stretches relatively far offshore in this northern area. For cruise M68/3, the offshore area with striking high NPP around 20° W might be fostered by the relatively large vertical nutrient transport observed at the two stations near 19° W. The reason for the high nutrient fluxes at this location is the above mentioned eddy induced upwelling. The stations near 18° W, 16.5° N are at least in close vicinity to the area with high NPP along the coast. For cruise P347 the calculated nutrient/carbon fluxes reflect the decrease of NPP in offshore direction. The limited number of stations with nutrient fluxes for ATA3 hamper to find a correlation with the underlying NPP field.

The spatial misfit between NPP and vertical nutrient supply might also be due to the temporal delay between them. Over this delay time, the upwelled water is advected horizontally, so NPP and nutrient flux are not expected to appear exactly at the same location. The lack of correlation between upwelling (local forcing) and primary production has also been found in a study by Carr and Kearns (2003). They analyzed the governing factors for the biological production in eastern boundary current systems and found even negative correlations between local forcing and primary production both for the northern part of the Humboldt Current off Peru (5–15° S) and the southern part of the Canary Current off Mauritania (11° S–20° N) (Carr and Kearns, 2003, Table 3).

The ~~vertical nutrient flux into the mixed layer should be more precisely compared with the net community production (NCP), which is NPP minus the respiration by autotrophs. From Fig. 10 it is obvious, that NCP is indeed larger than the equivalent vertical nutrient transport into the~~ important parameter for primary production is the nutrient flux at the base of the euphotic zone. This zone is typically deeper than the mixed layer for ~~most of the stations. The only exception are some stations from cruise M68/3 in the Mauritanian upwelling. One reason might be the above mentioned spatial and temporal mismatch between both~~

~~quantities. Also, for the primary production the nutrient flux at the base~~ which the fluxes in this study are calculated. However, neither the depth of the euphotic zone ~~is the important parameter, and this zone is typically~~ nore the vertical velocity w at this location is precisely known. Typically, the euphotic zone is deeper than the ~~mixed layer for which the fluxes in this study are calculated~~relatively shallow mixed layers observed in the upwelling regions. Assuming a decrease of w with depth and an increase of nutrient concentrations, these two gradients are counteracting in their effect on the nutrient flux, so the numbers presented here are considered as approximations of the nutrient flux in the euphotic zone.

Values for NCP in the Peruvian and Mauritanian upwelling have been calculated by Minas et al. (1986), $0.59\,\mathrm{g\,C\,m^{-2}\,d^{-1}}$ off Peru and $2.51\,\mathrm{g\,C\,m^{-2}\,d^{-1}}$ off Mauritania. For comparison, the regional mean values of the vertical carbon fluxes from this study are given in Table 3, divided into an diffusive and an advective part. As in Minas et al. (1986), the value for the Peruvian upwelling is smaller than for Mauritania (1.3 vs. 1.6~~–1.9~~–2.1 $\mathrm{g\,C\,m^{-2}\,d^{-1}}$), but the difference is much less pronounced.

The nutrient fluxes into the mixed layer by vertical advection and vertical mixing are of similar magnitude for the Peruvian offshore area and ~~the coastal~~ in most cases both for the coastal and offshore region off Mauritania. Over the Mauritanian shelf break, the vertical diffusivity is largely enhanced due to tide–topography interactions (Schafstall et al., 2010), which explains the high diffusive fluxes. Our result of ~~0.7~~0.8–0~~.8~~.9 $\mathrm{g\,C\,m^{-2}\,d^{-1}}$ is almost identical with the study in Schafstall et al. (2010) for the same region, but not exactly the same subset of cruises. Further offshore, the vertical diffusivity drops by more than one order of magnitude, which is not compensated by the slightly larger subsurface increase of nutrients in the offshore areas (Fig. 2d–f). This is different for the Peruvian region, where coastal and offshore diffusivities reach the same magnitude at some stations~~(see also Fig. 3), thus here~~. Here, the diffusive flux offshore is even higher than near the coast, and the coastal flux is dominated by the advective contribution. According to Carr and Kearns (2003), the open ocean productivity is ~~about~~ reduced by a factor of 10 ~~smaller than in~~ compared to the coastal upwelling areas. Such small values of vertical nutrient transport have been found in Haskell et al. (2015) further offshore off Peru ($0.01 - 0.1\,\mathrm{g\,C\,m^{-2}\,d^{-1}}$).

This indicates the transition from the upwelling regime towards the oligotrophic subtropical gyre. In the offshore regions adjacent to the coastal boundary analyzed here, the vertical nutrient transport is also smaller than ~~near~~ at the coast, but only by a factor of 1.3 (Peru, cruise M91) to 4 (Mauritania, cruise P347). The offshore filaments of enhanced productivity observed from satellite (Fig. ~~11~~8) might thus not only be fed by horizontal advection of nutrients out of the coastal zone, but also by nutrient input from below the mixed layer.

The general importance of eddies for the nutrient supply has been shown by Oschlies and Garçon (1998) in a model for the Atlantic. In another model study Gruber et al. (2011) show that the presence of eddies reduces the nutrient transport into the euphotic zone and thus the productivity in eastern boundary upwelling systems compared to the non-eddying case in the region adjacent to the coast (0–500 km). Further offshore (500–1000 km), however, the eddy field induces an increase in primary production and carbon export.

6 Conclusions

Vertical velocities w for the eastern boundary current upwelling systems off Peru and Mauritania regions have been determined by using the $^3He/^4He$ disequilibrium in surface waters. The mean upwelling velocity over the coastal regions varies between ~~1.1×10^{-5} and $2.8 \times 10^{-5}\,m\,s^{-1}$~~ $1.1 \pm 0.3 \times 10^{-5}$ and $2.4 \pm 1.5 \times 10^{-5}\,m\,s^{-1}$ and is similar for both regions. In the equatorial Atlantic Rhein et al. (2010) and Kadko and Johns (2011) found vertical velocities reaching from 0.6×10^{-5} to $2.6 \times 10^{-5}\,m\,s^{-1}$. Thus both the equatorial and the coastal upwelling are of similar strength.

For the Mauritanian area, Tanhua and Liu (2015) have calculated upwelling velocities using the same box model as here, but CFC-12 and SF_6 as tracers. For a winter and spring cruise, the vertical velocities are between 0 and $11 \times 10^{-5}\,m\,s^{-1}$, comparable with our results. For the summer cruise M68/3, Tanhua and Liu (2015) find no indications for upwelling. Their data set, however, only contains a few stations along 18° N. Our coastal stations along that line also have low vertical velocities (between 0 and

$2 \times 10^{-5}\,\mathrm{m\,s^{-1}}$), whereas directly north and around 20° N the helium derived upwelling exceeds $3 \times 10^{-5}\,\mathrm{m\,s^{-1}}$.

Haskell et al. (2015) investigate upwelling in the Eastern Tropical South Pacific at a few stations based on the ^{7}Be method. Their vertical velocities are also in the order of $10^{-5}\,\mathrm{m\,s^{-1}}$ ($0 - 3 \times 10^{-5}\,\mathrm{m\,s^{-1}}$), whereby the maximum value of $3 \times 10^{-5}\,\mathrm{m\,s^{-1}}$ might be due to 'anomalous ^{7}Be measurements'.

An independent estimate of the upwelling velocity can be inferred by Ekman theory (Gill, 1982). Near the coast, the agreement between wind and helium derived mean vertical velocities is fair, if a "minimum" water depth of 50 m for upwelling to occur is chosen. For the Peruvian upwelling, the vertical velocity derived from the helium method in conjunction with the gas exchange ~~parameterisation of Nightingale et al. (2000) might lead~~ parameterization of Nightingale et al. (2000) leads to an overestimation of the upwelling, as the gas exchange is reduced due to the presence of surface surfactants ~~. The deviation of the pointwise vertical helium and Ekman derived velocities can partially be explained by the large error of the helium method (81 % for the Peruvian and 98 % for the Mauritanian upwelling) and by additional sources of upwelling as flow–topography interaction (Mazzini and Barth, 2013) . If the main focus is on the mean coastal upwelling and not its local variations, it thus seems more practical to infer the coastal upwellingvelocities from the wind field. This avoids the uncertainties in the gas transfer velocity, and the data coverage is global with high temporal resolution~~(Kiefhaber at al., 2015) . Assuming a reduction of the piston velocity in the whole coastal area off Peru leads to a small underestimation of the upwelling, but helium and wind derived values still agree within their errors.

In contrast to the broad agreement between the mean upwelling derived from the helium and the wind method, at greater distances from the Mauritanian coast large discrepancies occur. Here, the helium derived upwelling still reaches $1 \times 10^{-5}\,\mathrm{m\,s^{-1}}$, whereas the wind driven upwelling from Ekman suction is smaller by ~~at least~~ upto one order of magnitude. Haskell et al. (2015) find an upward velocity of $1 \times 10^{-5}\,\mathrm{m\,s^{-1}}$ at 10° S, 100° W, which is another indication for enhanced upwelling in the open ocean. One possible mechanism is eddy induced upwelling by perturbations of the eddy flow field (Martin and Richards, 2001).

This view is supported by sea level anomalies, which are moderate at the locations of maximum upwelling, i. e. the largest upwelling is found at the edge of eddies and not in their center.

Vertical advection and diapycnal mixing are the most important mechanisms for the transport of substances from the interior ocean into the surface mixed layer. As a consequence, the upwelling regimes belong to the most productive ocean regions. Due to the high vertical diffusivities at the shelf break off Mauritania (Schafstall et al., 2010), in that area the diffusive nutrient flux is of the same magnitude as the advective one. Both type of fluxes together are equivalent to a carbon flux of ~~1.3~~$1.3 \pm 0.3\,\mathrm{g\,C\,m^{-2}\,d^{-1}}$ for the Peruvian and ~~1.6–1.9for the Mauritaniann~~ $1.6 - 2.1 \pm 0.5\,\mathrm{g\,C\,m^{-2}\,d^{-1}}$ for the Mauritanian region. The ~~eddy induced upwelling~~ upwelling also leads to enhanced nutrient fluxes ~~further offshore~~ in the offshore region, which can reach up to ~~1.0. This vertical nutrient supply might feed the offshore filaments of enhanced primary production. The general importance of eddies for the nutrient supply has been shown by Oschlies and Garçon (1998) in a model for the Atlantic. In another model study Gruber et al. (2011) show that the presence of eddies reduces the nutrient transport into the euphotic zone and thus the productivity in eastern boundary upwelling systems compared to the non eddying case in the region adjacent to the coast (0–500). Further offshore (500–1000), however, the eddy field induces an increase in primary production and carbon export. The main mechanism is an eddy driven offshore transport of nutrients, thus this effect would influence the nutrient concentration in the coastal and offshore region. These examples together with this study demonstrate the importance of eddies both for modulating the nutrient distribution below the mixed layer and for enhanced vertical exchange between the mixed layer and the subsurface waters~~ $1.5 \pm 0.4\,\mathrm{g\,C\,m^{-2}\,d^{-1}}$ off Mauritania during the cruise M68/3 and $1.0 \pm 0.1\,\mathrm{g\,C\,m^{-2}\,d^{-1}}$ off Peru for cruise M91.

Acknowledgements. This work is part of the German research project Surface Ocean Processes in the Anthropocene (SOPRAN), funded by the German Federal Ministry of Education and Research, BMBF, grants 03F0462D, 03F0611D, 03F0662D (M. Rhein, R. Steinfeldt, J. Sültenfuß) and grants 03F0462A, 03F0611A, 03F0662A (M. Dengler, T. Fischer). The authors thank captain and crews

of the cruises M91, M68/3, P347, and ATA3 for their professional field support. The wind speed data are derived from ftp://ftp.ifremer.fr/ifremer/cersat/products/gridded/mwf-ascat/data/daily and ftp://ftp.ifremer.fr/ifremer/cersat/products/gridded/mwf-quikscat/winds/daily for the time period of the Peruvian and Mauritanian cruises rspectively. The satellite data of primary production can be found at http://www.science.oregonstate.edu.ocean.productivity/index.php. The altimeter products were produced by Ssalto/Duacs and distribured by Aviso with support from CLS-Cnes (http://www.aviso.oceanobs.com/duacs/). The contribution from the group of Arne Körtzinger (GEOMAR), making the nutrient data available, is gratefully acknowledged. We also thank two anonymous reviewers for their valuable comments.

The article processing charges for this open-access publication were covered by the University of Bremen.

References

Anderson, L. A. A. and Sarmiento, J. L.: Redfield ratios of remineralization determined by nutrient data analysis, Global Biogeochem. Cy., 8, 65–80, 1994.

Behrenfeld, M. J. and Falkowski, P.-G.: Photosynthetic rates derived from satellite-based chlorophyll concentration, Limnol. Oceanogr., 42, 1–20, 1997.

Stanley, R. H. R, and Jenkins, W. J.: Chapter 4: Noble Gases in Seawater as Tracers for Physical and Biogeochamical Ocean Processes, in: Bernard, P. (ed.), The Noble Gases as Geochemical Tracers, Advances in Isotope Geochemistry, doi:10.1007/978-3-642-28836-4 SUBSCRIPTNB4, Springer-Verlag Berlin heidelberg, 2013.

Broecker, W. S., Peng, T. H., and Stuiver, M.: An estimate of the upwelling rate in the Equatorial Atlantic based on the distribution of bomb radiocarbon, J. Geophys. Res., 83, 6179–6186, 1978.

Carr, M.-E. and Kearns, E. J.: Production regimes in four Eastern Boundary Current systems, Deep-Sea Res. Pt. II, 50, 3199–3221, doi:10.1016/j.dsr2.2003.07.015, 2003.

Fennel, W.: Theory of the Benguela Upwelling System, J. Phys. Oceanogr., 29, 128–142, 1999.

Fréon, P., Barrange, M., and Aristegui, J.: Eastern boundary upwelling ecosystems: Integrative and comparative approaches, Progr. Oceanogr. 83, 1–14, 2009.

Gill, A. E.: Atmosphere-Ocean Dynamics, Academic Press, California, 662 pp., 1982.

Gruber, N., Lackhar, Z., Frenzel, H., Marchesiello, P., Münnich, M., McWilliams, J. C., Nagai, T., and Plattner, G.-K.: Eddy-induced reduction of biological production in eastern boundary upwelling systems, Nature Geosci., 4, 787–792, doi:10.1038/NGEO1273, 2011.

Gouriou, Y., and Reverdin, G.: Isopycnal and diapycnal circulation of the upper equatorial Atlantic Ocean in 1983—1984, J. Geophys. Res.,97(C3), 3543–3572, doi:10.1029/91JC02935, 1992.

Hagen, E.: Northwest African upwelling scenario, Oceanol. Acta, 23, S113–S124, ~~2000.~~ 2001.

Haskell, W. Z. II., Kadko, D., Hammond, D. E., Knapp, A. N. Prokopenko, M. G., Berelson, W. M., and Capone, D. G.: Upwelling velocity and eddy diffusivity from ^{7}Be measurements used to compare vertical nutrient flux to export POC flux in the Eastern Tropical South Pacific, Mar. Chem., 168, 140–150, doi:10.1016/j.marchem.2014.10.004, 2015.

Kadko, D. and Johns, W.: Inferring upwelling rates in the equatorial Atlantic using ^{7}Be measurements in the upper ocean, Deep-Sea Res. Pt. I, 58, 647–657, doi:10.1016/j.dsr.2011.03.004, 2011.

Karstensen, J., Stramma, L., and Visbeck, M.: Oxygen minimum zones in the eastern tropical Atlantic and Pacific oceans, Prog. Oceanogr., 77, 331–350, 2008.

Kiefhaber, D., Zappa, C. J., and Jähne, B.: Influence of natural surfactants on short wind waves in the coastal Peruvian waters, Ocean Sci. Discuss., 12, 1291-–1325, doi:10.5194/osd-12-1291-201, 2015.

Klein, B. and Rhein, M.: Equatorial upwelling rates inferred from helium isotope data: a novel approach, Geophys. Res. Lett., 31, L23308, doi:10.1029/2004GL021262, 2004.

Kock, A., Schafstall, J., Dengler, M., Brandt, P., and Bange, H. W.: Sea-to-air and diapycnal nitrous oxide fluxes in the eastern tropical North Atlantic Ocean, Biogeosciences, 9, 957–964, doi:10.5194/bg-9-957-2012, 2012.

Levitus, S.: Climatological Atlas of the World Ocean, NOAA Professional Paper 13, US Gov. Printing Office, Washington, DC, 117 pp., 1982.

Liss, P. S. and Merlivat, L.: Air-sea gas exchange rates: introduction and synthesis, in: The Role of Air-Sea Exchange in Geochemical Cycling, edited by: Buat-Ménard, P., D. Reidel, Norwell, Mass, 113–127, 1986.

Lupton, J.: Terrestrial inert gases – isotope tracer studies and clues to primordial components in the mantle, Annu. Rev. Earth Pl. Sc., 11, 371–414, 1983.

Martin, A. P. and Richards, K. J.: Mechanisms for vertical nutrient transport within a North Atlantic mesoscale eddy, Deep-Sea Res. Pt. II, 48, 757–773, 2001.

Mazzini, P. L. F. and Barth, J. A.: A comparison of mechanisms generating vertical transport in the ~~Brazlian~~ Brazilian coastal upwelling regions, J. Geophys. Res., 118, 5977–5993, doi:10.1002/2013JC008924, 2013.

McClain, C. R.: An Investigation of Ekman Upwelling in the North Atlantic, J. Geophys. Res., 98, C7, 12327–12339, 1993.

McGillicuddy Jr.,~~D.~~ D. J., Anderson,~~L.~~ L. A., Bates,~~N.~~ N. R., Bibby, T., Buesseler, K. O., Carlson,~~C.~~ C. A., Davis,~~C.~~ C. S., Ewart, C., Falkowski,~~P.~~ P. G., Goldthwait,~~S.~~ S. A., Hansell,~~D.~~ D. A., Jenkins,~~W.~~ W. J., Johnson, R., Kosnyrev,~~V.~~ V. K.,Ledwell,~~J.~~ J. R., Li,~~Q.~~ Q. P., Siegel,~~D.~~ D. A., and Steinberg,~~D.~~ D. K.: Eddy/wind interactions stimulate extraordinary mid-ocean plankton blooms, Science, 316, 1021–1026, doi:10.1126/science.1136256, 2007.

Minas, H. J., Minas, M., and Packard, T. T.: Productivity in upwelling areas deduced from hydrographic and chemical fields, Limnol. Oceanogr., 31, 1182–1206, 1986.

Nightingale, P. D., Malin, G., Law, C. S., Watson, A. J., Liss, P. S., Liddicoat, M. I., Boutin, J., and Upstill-Goddard, R. C.: In situ evaluation of air-sea gas exchange parameterizations using novel conservative and volatile tracers, Global Biogeochem. Cy., 14, 373–387, 2000.

Oakey, N. S.: Determination of the rate of dissipation of turbulent energy from simultaneous temperature and velocity shear microstructure measurements, J. Phys. Oceanogr., 12, 256–271, 1982.

Osborn, T. R.: Estimates of the local rate of vertical diffusion from dissipation measurements, J. Phys. Oceanogr., 10, 83–89, 1980.

Oschlies, A. and Garçon, V.: Eddy induced enhancement of primary pruduction in a model of the North Atlantic Ocean, Nature, 394, 266–269, 1998.

Prandke, H. and Stips, A.: Test measurements with an operational microstructure-turbulence profiler: Detection limits of diffipation rates, Aquat. Sci., 60, 191–209, 1998.

Quay, P.D., Stuiver, M., and Broecker, W. S.: Upwelling rates for the equatorial Pacific Ocean derived from the bomb ^{14}C distribution, J. Mar. Res. 41, 769–792,1983.

Rhein, M., Dengler, M., Sültenfuß, J., Hummels, R., Hüttl-Kabus, S., and Bourles, B.: Upwelling and associated heat flux in the equatorial Atlantic inferred from helium isotope disequilibrium, J. Geophys. Res., 115, C08021, doi:10.1029/2009JC005772, 2010.

Schafstall, J.: Turbulente Vermischungsprozesse und Zirkulation im Auftriebsgebiet vor Nordwestafrika, PhD thesis, IFM-GEOMAR, Universität, Kiel, Germany, 219 pp., 2010.

Schafstall, J., Dengler, M., Brandt, P., and Bange, H.: Tidal-induced mixing and diapycnal nutrient fluxes in the Mauritanian upwelling region, J. Geophys. Res., 115, C10014, doi:10.1029/2009JC005940, 2010.

Stramma, L., Bange, H. W., Czeschel, R., Lorenzo, A., and Frank, M.: On the role of mesoscale eddies for the biological productivity and biogeochemistry in the eastern tropical Pacific Ocean off Peru, Biogeosciences, 10, 7293–7306, doi:10.5194/bg-10-7293-2013, 2013.

Sültenfuß, J., Rhein, M., and Roether, W.: The Bremen mass spectrometer facility for the measurement of helium isotopes, neon, and tritium in water, Isot. Environ. Health S., 45, 1–13, 2009.

Tanhua, T., van Heuven, S., Key, ~~R.~~ R. M., Velo, A., Olsen, A., and Schirnick, C.: Quality control procedures and methods of the CARINA database, Earth Syst. Sci. Data, 2, 35–49, doi:10.5194/essd-2-35-2010, 2010.

Tanhua, T., and Liu, M.: Upwelling velocity and ventilation in the Mauritanian upwelling system estimated by CFC-12 and SF_6 observations, J. Mar. Sys., 151, 57–70, doi:10.1016/j.jmarsys.2015.07.002, 2015.

Toggweiler, J. R., Dixon, K., Broecker, W. S.: The Peru upwelling and the ventilation of the South Pacific thermocline, J. Geophys. Res. Oceans 96 (C11), 20467–20497, 1991

Tsai, W. T. and Liu, K. K.: An assessment of the effect of sea surface surfactant on global atmosphere-ocean CO_2 flux, J. Geophys. Res., 108, 3127, doi:10.1029/2000JC000740, 2003.

Wanninkhof, R., Feely, R. A., Atwood, D. K., Berberian, G., Wilson, D., Murphy, P. P., Lamb, M. F.: Seasonal and lateral variations in carbon chemistry of surface water in the eastern equatorial Pacific during 1992. Deep-Sea Res. II 42, 387–409.

Weingartner, T. J., and Weisberg, R. H.: On the annual cycle of equatorial upwelling in the central Atlantic ocean, J. Phys. Oceanogr., 21, 68–82, 1991.

Yoshida, K.: Coastal upwelling off the California coast, Records Oceanogr. Works Japan, 2, 8–20, 1955.

Table 1. Error estimation.

	δ^3He box 1	δ^3He box 2	vert. mixing	~~wind speed~~ piston velocity
uncertainty	±0.2 %	~~±0.25 %~~ ±0.2 %	factor of 2	~~SD of daily winds (≈ 10 %)~~ 30
error of w_{He} Peru	~~±81 %~~ ±22 %	~~±19 %~~ ±17 %	±42 %	~~±30 %~~ ±46
error of w_{He} Maur.	~~±47 %~~ ±42 %	~~±12 %~~ ±26 %	~~±44 %~~ ±64 %	~~±48 %~~ ±59

Table 2. Mean upwelling velocities w.

	M91			M68/3		P347	
	coastal	coastal surf.	offshore	coastal	offshore	coastal	offshore
♯ prof. $w > 0$	14	12	~~14~~ 12	5	~~10~~ 8	~~19~~ 17	4
♯ prof. $w \leq 0$	5	7	~~16~~ 18	3	~~7~~ 9	11	6
w_{Helium} $[10^{-5}\,\text{m}\,\text{s}^{-1}]$	2.7 ± 0.6	~~1.1 ± 0.3~~ 1.0 ± 0.3	0.6 ± 0.2	~~2.1 ± 0.8~~ 2.1 ± 0.7	~~1.0 ± 0.4~~ 0.7 ± 0.3	1.4 ± 0.4	0.2 ± 0.1
w_{Wind} $[10^{-5}\,\text{m}\,\text{s}^{-1}]$	~~1.2 ± 0.2~~ 1.3 ± 0.2	–	0.4 ± 0.1	3.7 ± 1.7	0.3 ± 0.1	1.2 ± 0.3	0.02 ± 0.01

Table 3. Mean advective, diffusive, and total PO_4 fluxes into the mixed layer converted to carbon units [g C m^{-2} d^{-1}] via the Redfield ratio.

	M91		M68/3		P347		
	coastal	offshore	coastal	offshore	coastal	offshore	
adv.	1.0 ± 0.3	~~0.5 ± 0.1~~ 0.4 ± 0.1	1.1 ± 0.4	~~1.0 ± 0.4~~ 0.7 ± 0.3	0.8 ± 0.3	0.2 ± 0.1	
diff.	0.3 ± 0.1	0.5 ± 0.1	~~0.7 ± 0.2~~ 0.9 ± 0.2	~~0.5 ± 0.1~~ 0.9 ± 0.2	0.8 ± 0.4	0.2 ± 0.1	~~0.8 ± 0.3~~
total	1.3 ± 0.3	~~1.0 ± 0.1~~ 0.9 ± 0.1	~~1.9 ± 0.5~~ 2.1 ± 0.5	~~1.5 ± 0.4~~ 1.6 ± 0.4	1.6 ± 0.5	0.4 ± 0.1	

For cruise ATA3, no advective nutrient flux for the coastal area has been computed. Only one station with helium and phosphate data for that region sufficient to calculate a mean value.

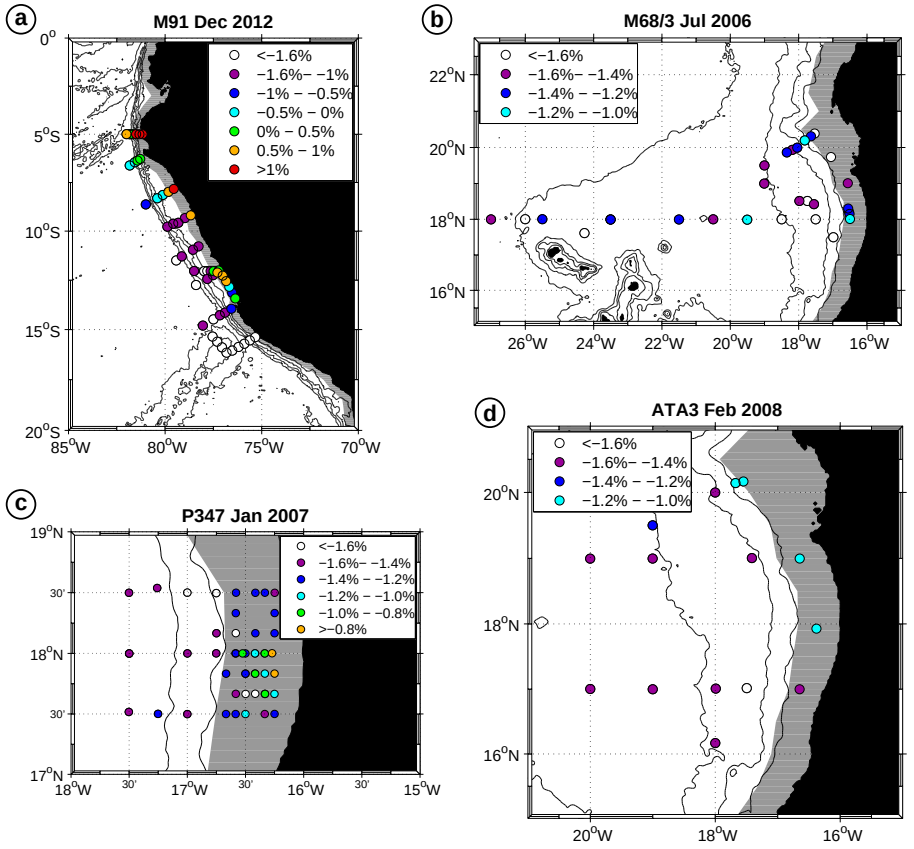

Figure 1. δ^3He [%] in the mixed layer for cruise M91 off Peru **(a)** and for cruises M68/3, P347 and ATA3 off Mauritania **(b–d)**. Isobaths are drawn every 1000 m, and the area ~~shallower than 500 m~~ of the 'coastal region' is shaded grey (for details, see text). Note the different color scale for the ~~crusies~~ cruises from the Peruvian **(a)** and Mauritanian **(b–d)** region. The error of the δ^3He values in the mixed layer is 0.2 %.

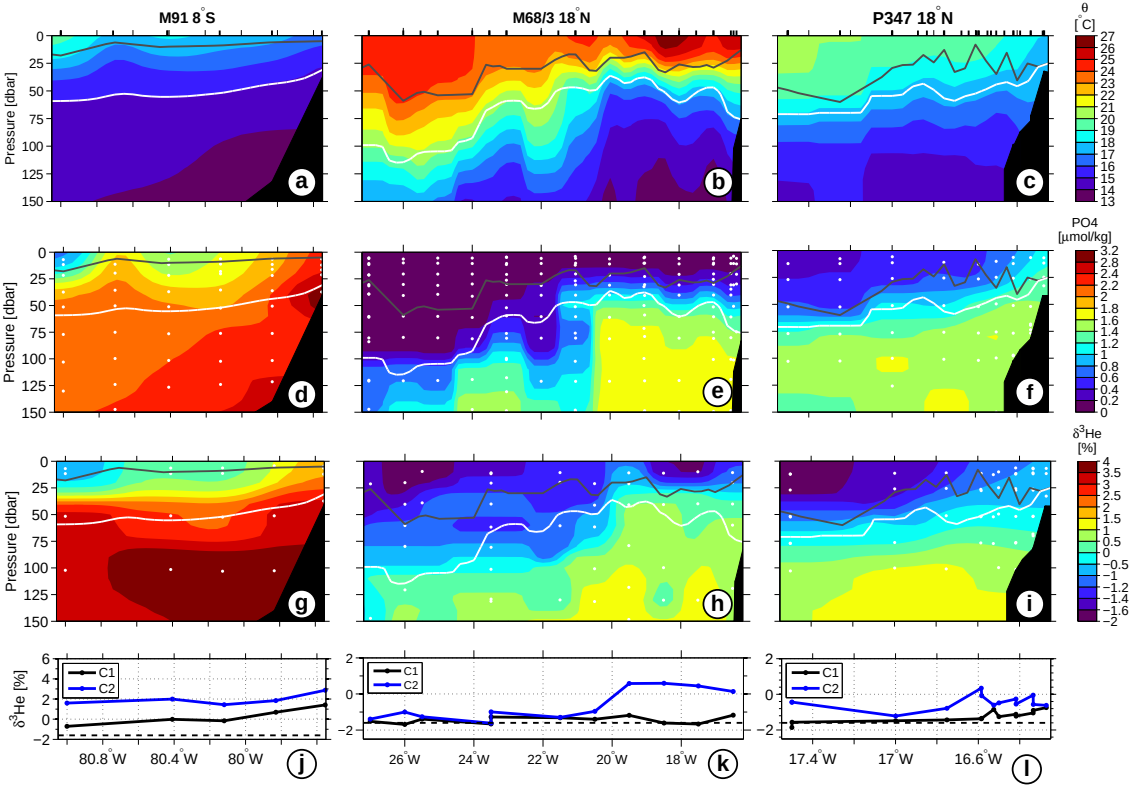

Figure 2. Sections of potential temperature **(a–c)**, phosphate **(d–f)**, helium 3 **(g–i)** for one section from cruise M91 off Peru (along 8° S), M68/3 (along 18° N) and P347 (also along 18° N). The grey line denotes the base of the mixed layer and the white line the isopycnal $\sigma_\theta = 26.0\,\mathrm{kg\,m^{-3}}$. **(j–l)**: mean δ^3He in box 1 (mixed layer) and box 2 (5–25 m below the mixed layer) along the sections.

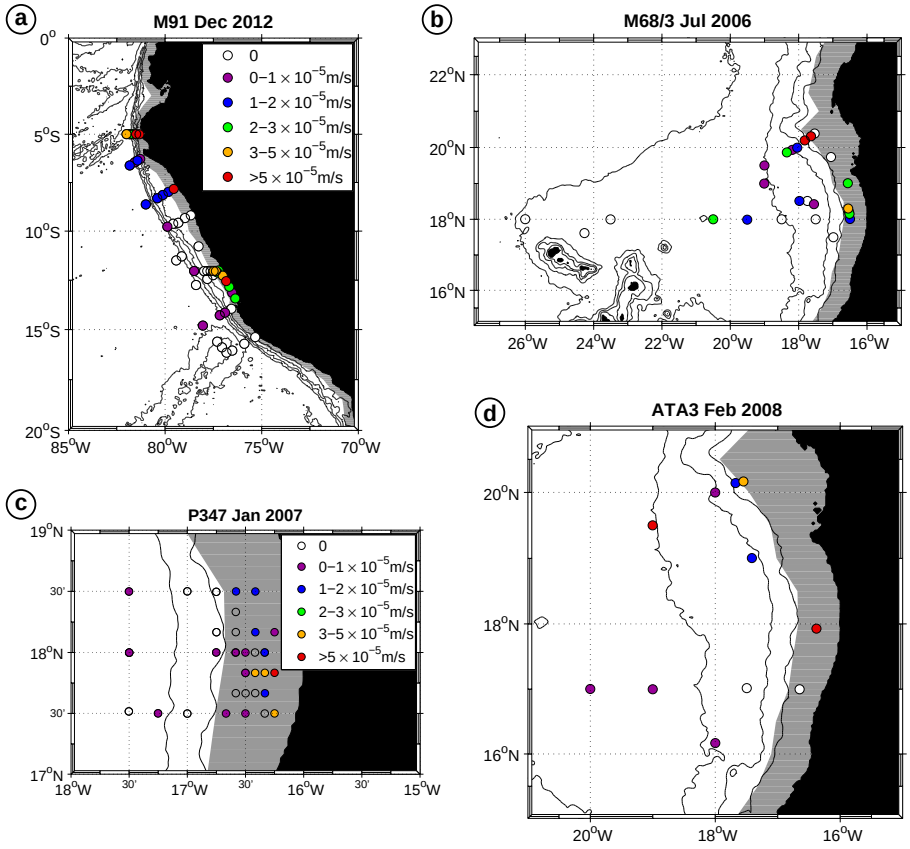

Figure 3. ~~Measured vertical diffusivity k_v vs. water depth~~ Helium derived upwelling velocities for ~~cruises~~ cruise M91 ~~,~~ off Peru **(a)** and for cruises M68/3, P347 and ATA3 off Mauritania **(b–d)**. ~~The black line is a linear fit between k_v~~ Isobaths are drawn every 1000 m, and the ~~logarithm~~ area of the ~~water depth~~'coastal region' is shaded grey. Note that the uncertainty of the pointwise helium derived upwelling velocities is 68 % for the Peruvian and 100 % for the Mauritanian data (for details, see text).

Helium derived upwelling velocities for cruise M91 off Peru **(a)** and for cruises M68/3, P347 and ATA3 off Mauritania **(b–d)**. Isobaths are drawn every 1000 m, and the area shallower than 500 m is shaded grey.

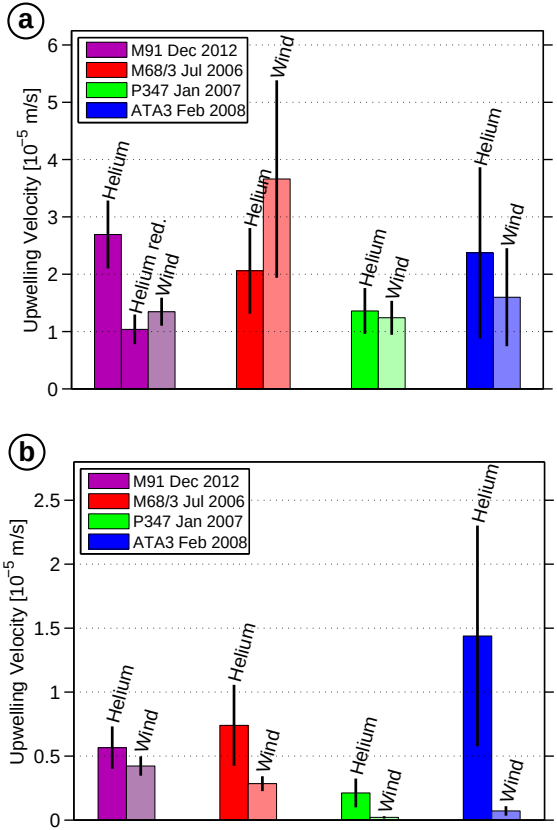

Figure 4. Mean values of helium and wind derived upwelling velocities for the coastal **(a)** and offshore **(b)** areas of cruises M91, M68/3, P347 and ATA3. The vertical black line indicates the standard deviation of the mean. “Helium red.” in **(a)** means that the helium derived upwelling is calculated with reduced gas exchange velocity due to the presence of surface organic films, for details see text.

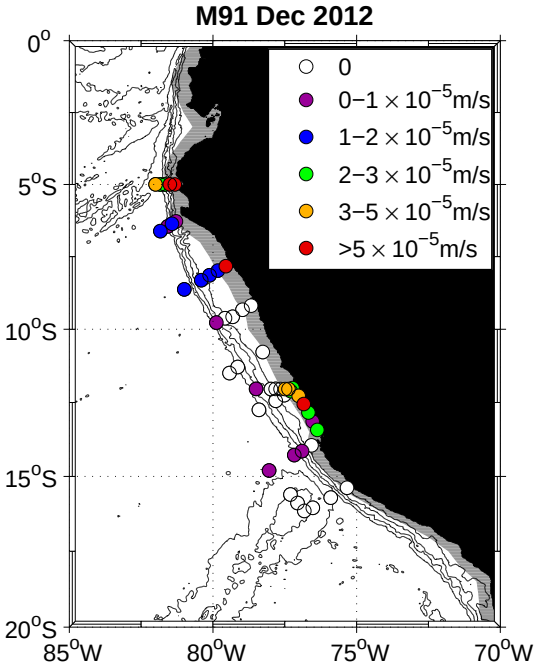

Figure 5. Helium derived vertical velocity for cruise M91. As in Fig. 3a, but applying a reduced gas transfer velocity in the coastal area due to the presence of surface films~~, for detals see text~~.

~~Comparison of helium and wind derived upwelling velocities for the coastal (filled circles) and offshore (open circles) areas of cruises M91, M68/3, P347 and ATA3.~~

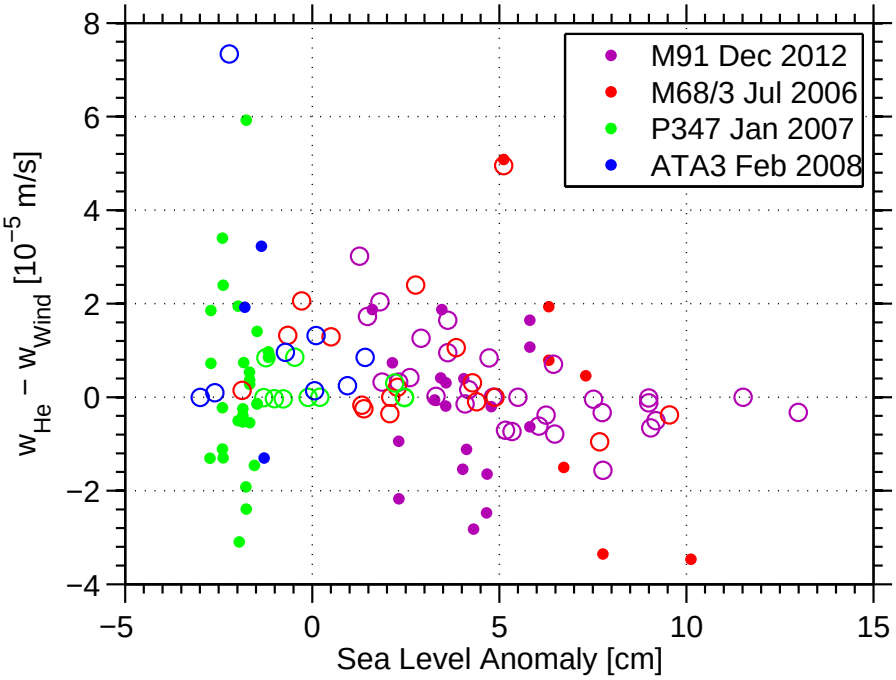

Figure 6. ~~Helium derived vertical velocity agains sea level anomaly at each stations for the coastal (filled circles) and offshore (open circles) region of cruises M91, M68/3, P347 and ATA3.~~ Difference between helium and wind derived vertical velocity against sea level anomaly at each stations for the coastal (filled circles) and offshore (open circles) region of cruises M91, M68/3, P347 and ATA3. Note that the uncertainty of the helium derived upwelling velocities is 68% for the Peruvian and 100% for the Mauritanian data.

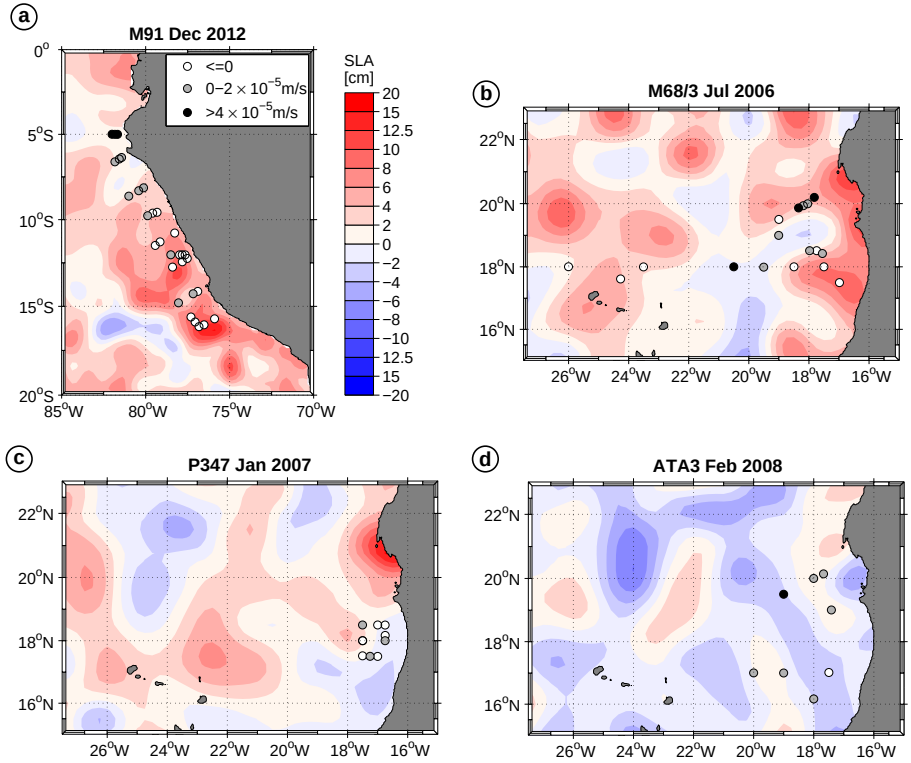

Figure 7. Mean sea level anomaly over the time period of the respective cruise for M91 **(a)**, M68/3 **(b)**, P347 **(c)**, and ATA3 **(d)**. The difference between helium and wind derived vertical velocity is indicated by the grey dots. For details see text.

~~Vertical phosphate transport into the mixed layer (advective plus diffusive part, converted to carbon units via the Redfield ratio) vs. satellite observed net primary production at each stations for the coastal (filled circles) and offshore (open circles) region of cruises M91, M68/3, P347 and ATA3.~~

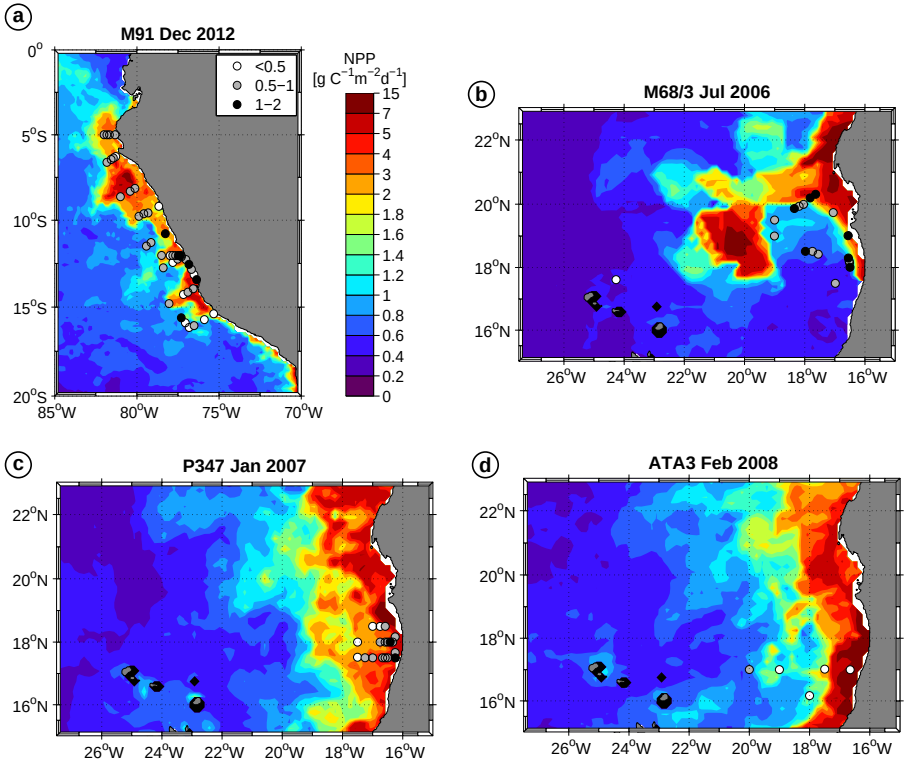

Figure 8. Mean net primary production over the time period of the respective cruise for M91 **(a)**, M68/3 **(b)**, P347 **(c)**, and ATA3 **(d)**. The vertical phosphate transport (advective plus diffusive part) into the mixed layer is converted to carbon units by the Redfield ratio and indicated by the grey dots. Note that the error of these fluxes is 100 %. For details see text.